AD-A127 515 ELECTROMAGNETIC MIRROR DYNAMICS(U) AIR FORCE INST OF TECH WRIGHT-PATTERSON AFB OH SCHOOL OF ENGINEERING R K HILL DEC 82 AFIT/GEP/PH/82D-13 1/1

UNCLASSIFIED F/G 20/7 NL

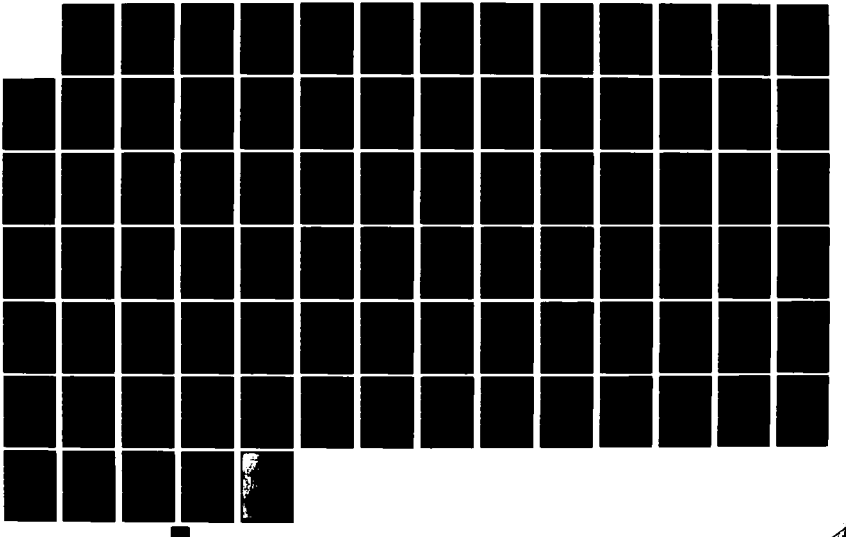

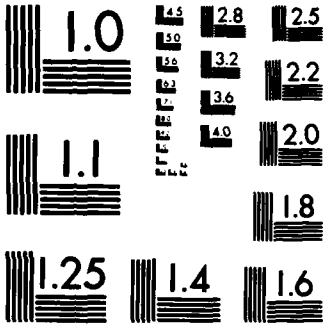

ELECTROMAGNETIC MIRROR DYNAMICS

THESIS

AFIT/GEP/PH/82D-13 Richard K. Hill
Capt USAF

DEPARTMENT OF THE AIR FORCE
AIR UNIVERSITY (ATC)
AIR FORCE INSTITUTE OF TECHNOLOGY

Wright-Patterson Air Force Base, Ohio

AFIT/GEP/PH/82D-13

ELECTROMAGNETIC MIRROR DYNAMICS

THESIS

AFIT/GEP/PH/82D-13 Richard K. Hill
Capt USAF

Approved for public release; distribution unlimited.

AFIT/GEP/PH/82D-13

ELECTROMAGNETIC MIRROR DYNAMICS

THESIS

Presented to the Faculty of the School of Engineering
of the Air Force Institute of Technology
Air University
in Partial Fulfillment of the
Requirements for the Degree of
Master of Science

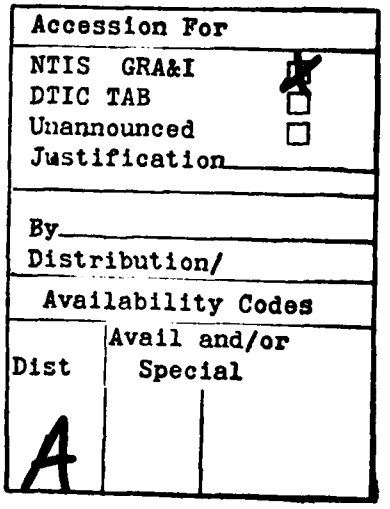

by

Richard K. Hill, B.S.
Capt USAF
Graduate Engineering Physics

December 1982

Approved for public release; distribution unlimited.

Acknowledgements

I would like to acknowledge the guidance and assistance of Dr. Richard Cook, who provided the impetus for this thesis, and without whose help, completion would have been very difficult. I would also like to acknowledge the help and encouragement of Dr. Leno Pedrotti and the assistance of the AFIT Library Staff. The MACSYMA Computer facility at MIT is also deserving of my thanks, for without their programs some of the calculations in this thesis would have been impossible. Finally, I must acknowledge the support and assistance of my fiancee, Susan Scott. Her understanding support and typing ability were vital to the completion of this thesis.

Richard K. Hill

Contents

List of Figures

Abstract

The phenomena of resonant radiation pressure is studied as it applies to the reflection of two-level atoms from an evanescent wave. The basic mechanism is examined in detail. Three applications are proposed, analyzed, and compared to existing methods of neutral beam control. The first application is a beam conducting pipe which can contain and decelerate a beam of atoms. The second application is a parabolic nozzle which can collimate and focus a beam three orders of magnitude better than comparable resonant focusing. The third application is a macroscopic trap for slow atoms which allows laser-free observation of ~100cm/s atoms for times measured in seconds. A computer code which tracks atomic trajectories through multiple reflections is included.

ELECTROMAGNETIC MIRROR DYNAMICS

I. Introduction

Background

Beams of neutral particles are extremely useful for studying many physical phenomena such as natural fluorescence and neutral particle scattering. Until recently, the only effective means of manipulating neutral beams was with slits and baffles, or (where possible) by inducing a dipole in the atoms. Both of these methods have very limited applications.

Resonant radiation pressure has been used in the last ten years for limited control of neutral beams (Refs 1-7). This pressure is a quantum-mechanical force which occurs when a strong laser beam strikes the beam of atoms. The pressure can be used to deflect (Refs 1-3), focus (Ref 5), and accelerate (Refs 7-8) a beam of atoms. Atomic trapping schemes have been proposed (Refs 9-13) but not demonstrated. All of these applications have used laser beams which propagate through a vacuum and directly strike the atomic beams.

The direct contact of the atomic and laser beams imposes two limitations, the first is due to different atomic speeds in the beam, which causes Doppler shifts and greatly affects the strength of the resonant radiation pressure.

The second limitation is due to the continuous pressure needed in any trapping scheme. This means that the atoms are constantly in the laser beam and affected by it. Observation of trapped atoms unaffected by the laser is highly desirable for very accurate spectroscopy (Ref 7).

A new arrangement for using resonant radiation pressure has been developed which involves the total internal reflection of the laser beam. This reflection creates a thin (~10 micron) evanescent wave above the reflecting surface which could be used to deflect a resonant neutral beam. The atoms would only be in the radiation for a short time, and this would allow unaffected observation of the atoms if a proper mirror geometry could be found. The mirror could also be curved and arranged to focus and manipulate a beam.

This new arrangement has many possibilities, but this type of reflection is very different from standard elastic reflection. The direction of the reflected atomic beam depends on its incident speed and direction. It also depends on the reflection angle of the laser beam. In addition, the strength of reflection (how much of the beam will reflect) is very sensitive to the speed and direction of the atomic beam and the frequency and direction of the laser. No systematic investigation of these factors has been made.

Problem Statement

Evanescent resonant reflection is investigated in order to find applications in the control of neutral atomic and molecular beams. The investigation focuses on overcoming the unusual nature of the reflection and using the inherent properties to advantage. Applications in beam conduction, intensity enhancement, and macroscopic trapping are developed and discussed.

Assumptions

Several assumptions are used in this thesis. First, only slow (~1000cm/s) beams of atoms are considered. This is explained under the Basic Mechanism section and is due to the weak nature of the reflection. Beam chopping is envisioned to eliminate the unwanted high velocity portion of the beam. Second, quantum fluctuations in the force are only treated approximately. A full treatment of these fluctuations is beyond the scope of this thesis. Finally, atom-atom interactions are ignored due to the tenuous nature of the beams used in current research. Further limited assumptions are identified as they are used.

Scope

This thesis studies the ideal reflection of an atomic beam by a near-resonant evanescent wave. Well collimated (.01 radian) beams are considered throughout. A thermal velocity distribution is considered (modified by current

deceleration techniques where applicable), or chopped to discard the high velocity atoms. Gravity is considered throughout due to its large effect on slow trajectories. Only physically realizable wave fronts and intensities (~1watt/cm^2) are considered. Doppler detuning of the force is considered, as well as atomic transitions out of resonance with the laser beam. These factors limit the intensity and length of application of the force.

Summary of Current Knowledge

At present there are no published works which deal with this exact problem, although there are many in the basic area of resonance-radiation pressure; and "the subject of atomic motion in resonant radiation is now a rapidly developing field of research" (Ref 14). Dr. Richard Cook of the AFIT faculty developed the idea of using an evanescent wave in conjunction with the resonant pressure to create an effective mirror for atoms. A good deal of time was spent rederiving and verifying his initial results. These results are presented in Appendix A in the form of a joint article which has been accepted for publication in Optics Communications.

The theory of resonant radiation pressure dates back to 1917 with a paper of Einstein titled "The Quantum Theory of Radiation" (Ref 15). The force was first observed by Frish (Ref 16) in 1933. The advent of tunable lasers

renewed interest in the force, and much theoretical development (Refs 17-24) and experimental verification (Refs 1-7) followed.

The latest interest in the field has centered on isotope separation (Ref 2), beam deceleration (Ref 7), and the trapping of single atoms (Refs 10-13). This thesis presents (1) new avenues in the last two areas and (2) hope in general beam control techniques.

Approach

This thesis is an extension of the results presented in Appendix A. Several promising geometries were investigated for atomic beams, reflecting surfaces and incident radiation. The geometries which have practical applications to beam control or confinement are presented. The results presented are by no means exhaustive of the possible geometries, but every effort was given to finding the most practical applications. Any lack of completeness is due to oversight, as a logical approach was taken in designating promising geometries.

The basic mechanism of evanescent reflection is examined first. This is a straightforward extension of Appendix A, with an eye to limitations on the force due to beam parameters and reflector geometry.

An analysis of a single reflection from a plane surface is presented second. The emphasis here is to develop the single bounce velocity effects on atoms in the beam.

Third, a beam conducting pipe is imagined and examined as a transverse folding of the plane surface around the beam to contain and channel the beam.

Completely enfolding the beam and making the reflector parabolic results in a nozzle which can greatly enhance the beam intensity with little adverse effect. This is explained in the fourth section of the development.

Fifth, the extension of the transverse confinement of the beam conducting pipe to a longitudinal confinement leads to a macroscopic trap for slow atoms (~200cm/s). This could have direct application in the field of Doppler-free atomic spectroscopy.

Finally, the results obtained are compared and contrasted to similar results for beam control and trapping in the current literature.

The BASIC program used to test the thesis results is presented in Appendix B to aid subsequent research. This program follows the trajectory of an atom through multiple bounces off three-dimensional surfaces which are illuminated by very general laser fields.

II. Development of the Dynamics of an Electromagnetic Mirror

Basic Mechanism

The quantum mechanical derivation of the forces involved in evanescent reflection is given in Appendix A and is summarized below. The situation is as shown in Figure 1. However, note that the axes are labeled differently in the appendix. This is to standardize the notation when gravity is included in this discussion. The interaction is between a single freely moving atom and a near-resonant evanescent wave.

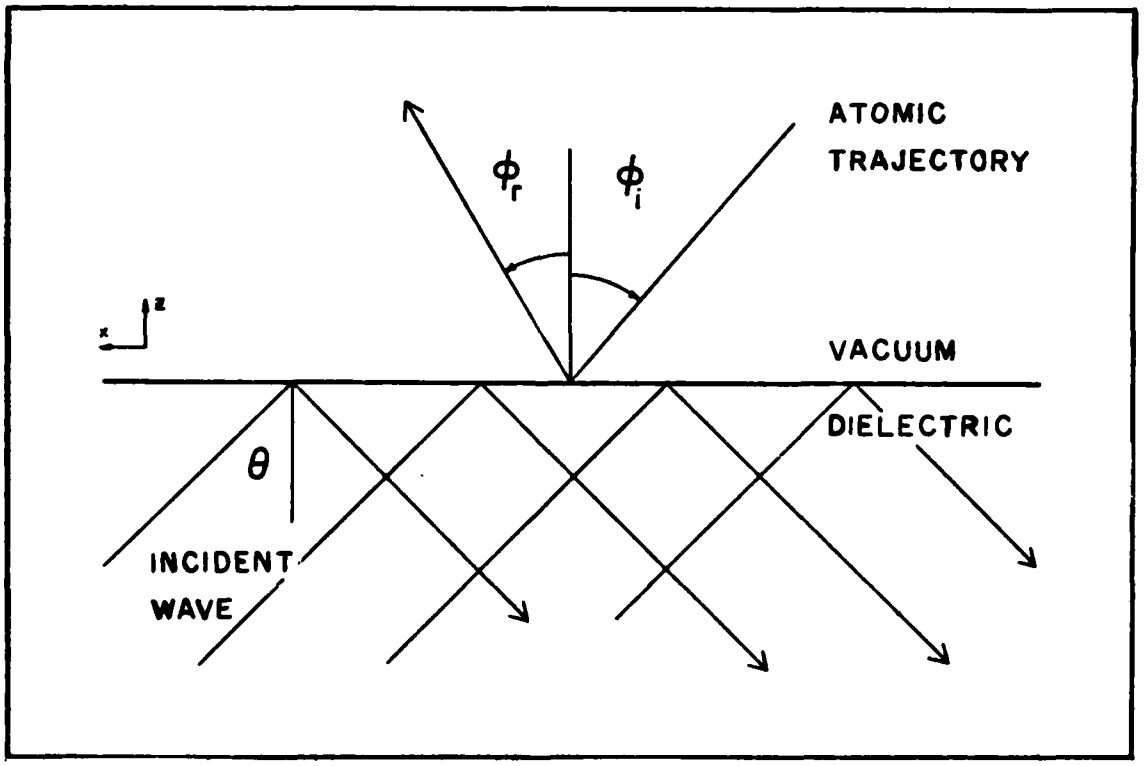

Figure 1. Geometry of Basic Interaction

The atom is assumed to have only two internal quantum states and is subject to no other external forces during the interaction. These two assumptions are valid for most systems of interest. The requirement of only two quantum states can be approximated for many atoms and molecules (Ref 25). In a number of cases, this requirement can be achieved by the proper choice of the transition. Another method is to apply a magnetic field to Zeemann shift the transitions and discriminate against optical pumping of the atom out of resonance. Results on sodium atoms (Ref 7) have shown that unwanted transition rates can be reduced to $\sim 10^{-4}$ times the rate of the desired transition. This figure will be used to assess the limitations of the force.

The neglect of nonelectromagnetic forces during the interaction is very easy to justify. In a normal interaction, the atom is affected by the field for a very short time due to the nature of the evanescent wave.

For an incident laser intensity of one watt/cm^2, and a representative reflection, the atom undergoes ~320 spontaneous emissions. This is accomplished in ~5μs. During this time, gravitational acceleration is negligible and the effect of a locally applied magnetic field for Zeemann shifting can be easily ignored.

The evanescent wave is also fairly easy to achieve. It arises from the total internal reflection of a tunable laser beam from a dielectric interface. This beam can be

introduced into the dielectric through normal incidence on a surface and directed toward the reflecting surface. In addition, the laser beam can make numerous internal reflections by bouncing off dielectric surfaces. Consequently, a single beam can be made to illuminate a large area of the reflecting surface with undiminished intensity. This arrangement is used in all of the applications which follow. The only losses in this type of system are due to absorption in the dielectric, imperfections on the surfaces, and the momentum transfer to the reflected atoms.

For a plane electromagnetic wave of frequency ω propagating in a dielectric of refractive index n, the evanescent wave will have the form

$$\vec{E}(\vec{x},t) = \hat{\varepsilon}\xi e^{-\alpha z}\cos\{\omega t - kx\} \qquad (1)$$

where $\hat{\varepsilon}$ = the unit polarization vector,

ξ = wave amplitude at z=0,

$\alpha = \omega(n^2\sin^2\theta - 1)^{\frac{1}{2}}/c$,

$k = \omega n\sin\theta/c$,

and θ = angle of incidence.

The interaction consists of two forces. The first gives rise to the zero-order effect: the reflection. This is the force normal to the surface, and is given by

$$F_z = \frac{2\alpha\hbar(\Delta - kv_x)\Omega^2(z)}{4(\Delta - kv_x)^2 + A^2 + 2\Omega^2(z)} \qquad (2)$$

where $\Delta = \omega - \omega_o$ (detuning)

$\Omega = \mu\xi\exp(-\alpha z)/\hbar$ (Rabi frequency)

$A = 4\mu^2\omega_o^3/3\hbar c^3$ (Einstein A coefficient)

ω_o = atomic transition frequency

and μ = dipole transition moment.

Note that for reflection this force must be positive, necessitating a positive Δ. That is, the laser must be tuned above the transition frequency of the atom.

The second force is parallel to the surface and in the direction of the evanescent wave vector. This force is given by

$$F_x = \frac{\hbar k A \Omega^2(z)}{4(\Delta - kv_x)^2 + A^2 + 2\Omega^2(z)} \qquad (3)$$

This is the first-order effect of the reflection, and serves to give an added "kick" to the atom in the direction of the evanescent wave vector. It is this force which can be used to decelerate or redirect parts of an atomic beam. It is a hinderance, however, in collimation and trapping.

Two important results follow from Eqs (2) and (3). The first gives the maximum normal velocity which can be reflected. This is the major limitation on the force and is given by

$$v_z^{max} = \{\frac{\hbar\Delta}{M} \ln(1 + \frac{2\mu^2\xi^2}{\hbar^2[4(\Delta - kv_x)^2 + A^2]})\}^{\frac{1}{2}} \qquad (4)$$

where M is the mass of the atom, and Δ' includes doppler effects. The second result directly relates the strength of the kick to the strength of the reflection. The ratio of these two forces is designated R, and is given by

$$R = \frac{F_x}{F_z} = \frac{kA}{2\alpha\Delta'} = \frac{nA\sin\theta}{2\Delta'(n^2\sin^2\theta-1)^{\frac{1}{2}}} \qquad (5)$$

This ratio is independent of position which means that the atom will always experience a kick which is proportional to its initial velocity normal to the surface.

To get a feel for these two results, consider the case of a sodium atom utilizing the standard $3^2S_{1/2}\rightarrow 3^2P_{3/2}$ transition. Then $M = 3.817\times10^{-23}g$, $\omega_o = 5.090\times10^{14}s^{-1}$, $A = 6.22\times10^{7}s^{-1}$, and $\mu = 1.003\times10^{-16}$. Using a nominal laser irradiance $I = 1watt/cm^2$, the field strength ξ, and the Rabi flopping freuqency Ω depend only on the refractive index n and the angle of incidence θ of the laser. Plots of

$$\xi^2 = 128\pi n^2\cos^2\theta I/(n^2-1)(n+1)^2c \qquad (6)$$

and

$$\Omega_o = \mu\xi/h \qquad (7)$$

are shown in Figure 2 for various values of n and θ (Ω_o is the Rabi frequency at z=0). For the purposes of this thesis, values of n=1.5 and $\theta=45^o$ give a good trade-off between available dielectric media and low angles of incidence. A

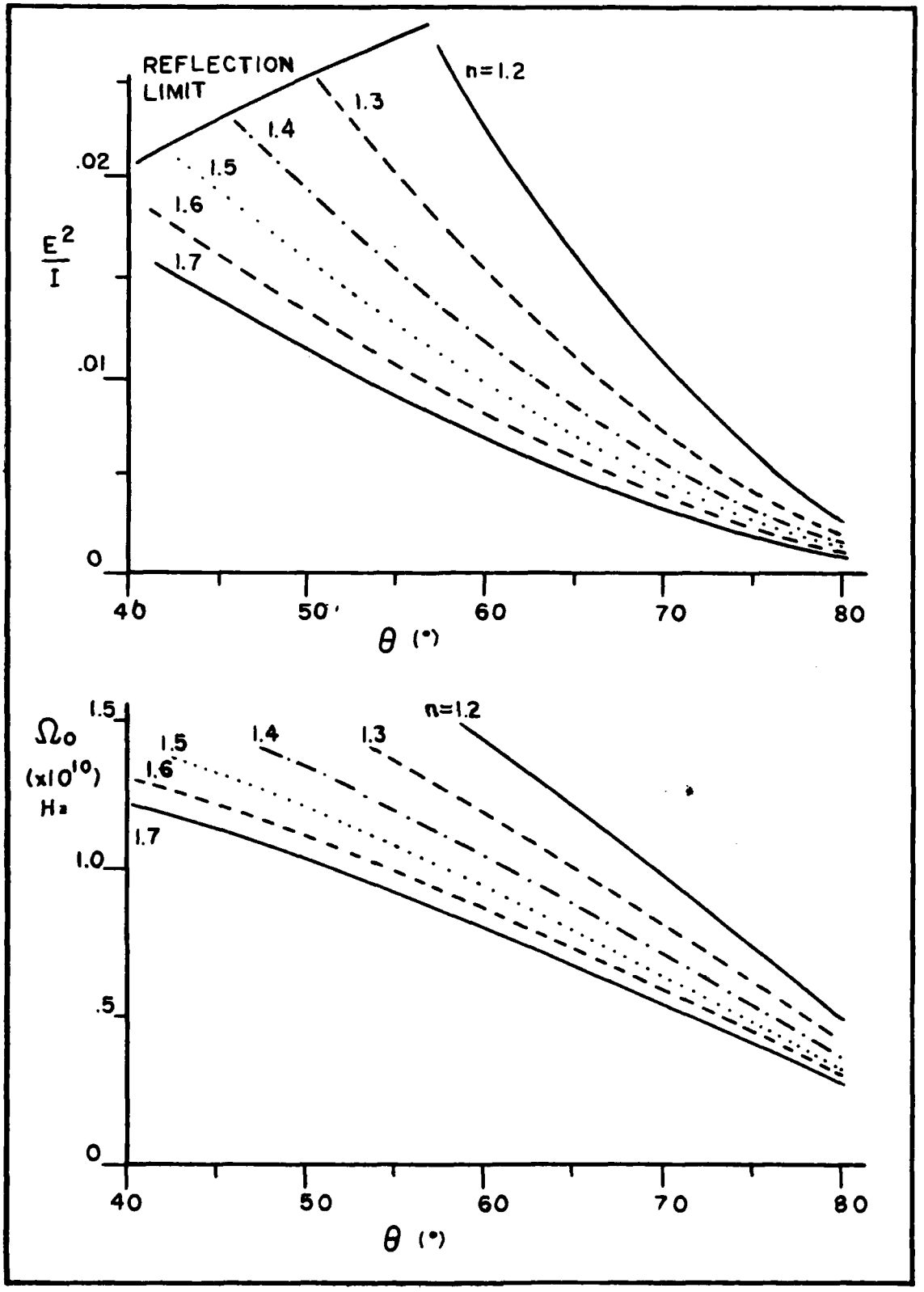

Figure 2. Dependence of E squared and Ω_o

low angle of incidence is desirable for multiple reflections as outlined earlier.

With n and θ fixed, the maximum normal velocity and the kick ratio depend only on the detuning Δ (plus doppler effects). Plots of this dependence are given in Figure 3. The figure is split into low and high detuning regimes to show the ranges for maximum kick and reflection. Because Doppler effects must be considered in the detuning, uncertainties are shown for both regimes appropriate to the expected range of longitudinal velocities (after velocity selection). Nominal detuning values of $5x10^8 s^{-1}$ for a moderate kick and $5x10^9 s^{-1}$ for reflection of maximum normal velocity will be used henceforth.

Plane Mirror Analysis

Semi-Classical Effect. The easiest case of electromagnetic reflection to analyze is that of simple reflection from a plane surface. Therefore, consider a dielectric interface illuminated from within by a plane wave as shown in Figure 1. Atoms in the beam which have a normal velocity component less than the maximum (υmax) dictated by I, n, θ, and Δ will be reflected with an equal (but opposite) normal component. During this reflection, however, they will gain (or lose) momentum from the spontaneous interaction with the field. This momentum will be gained parallel to the interface and in the direction of the k-vector of the evanescent wave.

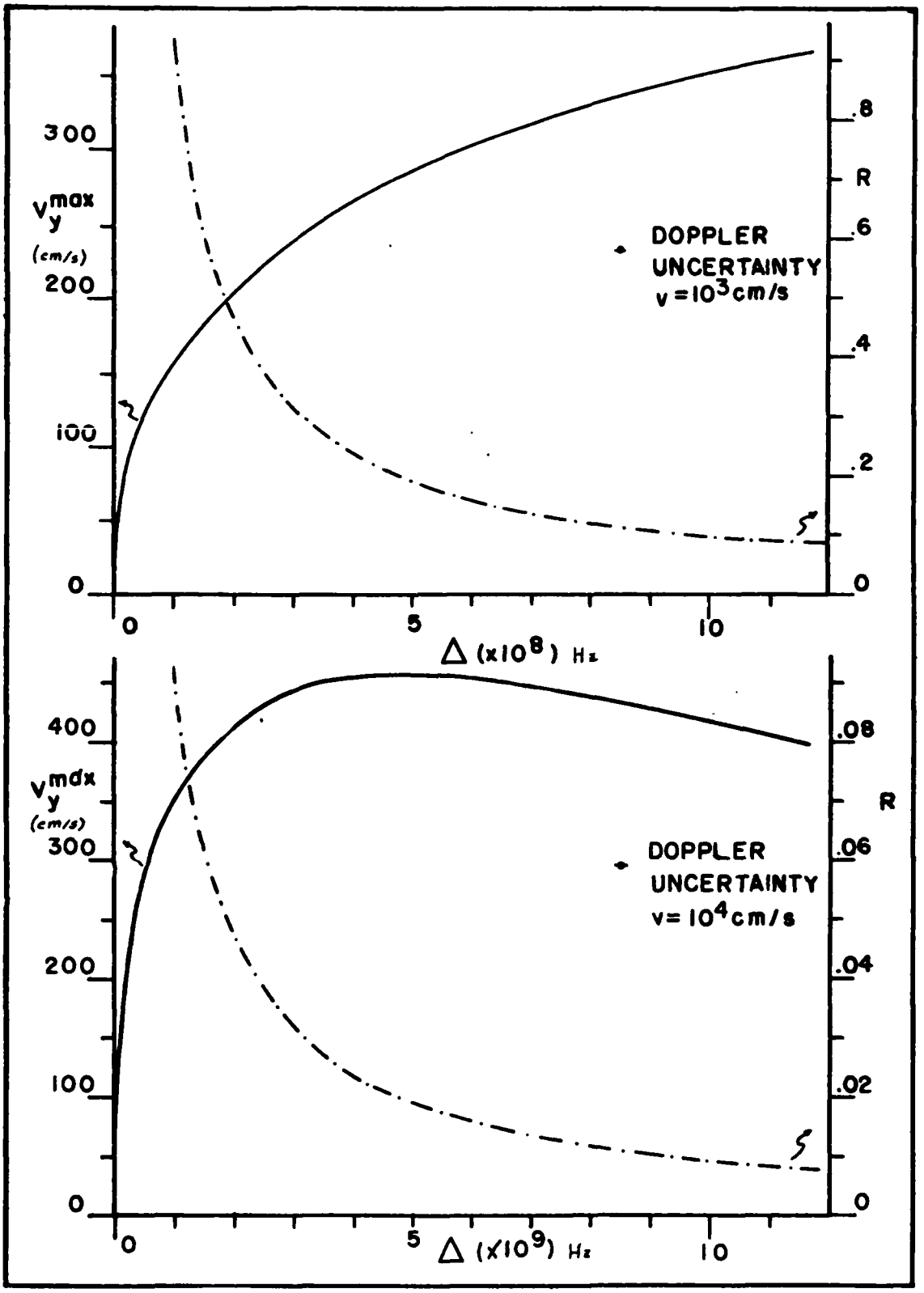

Figure 3. Dependence of v max and R for Sodium

For counter-directed radiation, this will slow all atoms which are reflected. For an ideal beam of thermal velocity distribution and grazing incidence at angle ϕ, the results are as follows. All atoms with velocity less than $\upsilon max/sin\phi$ will be reflected. Atoms with velocities greater than this value will strike the dielectric interface and either be absorbed, scattered elastically, or inelastically.

Atoms which are absorbed or inelastically reflected will damage the surface. Elastically scattered atoms will lose a momentum increment proportional to the time they interact with the field. This is a complex function roughly inversely proportional to the atom's initial velocity. No reliable estimate of the number of elastically scattered atoms is possible; therefore, atoms with normal velocities greater than υmax will be omitted from further consideration, except as a limit to the interaction.

Atoms with velocities less than υmax will be reflected by the evanescent wave. In addition to a reversal of their initial normal velocity, these atoms will lose longitudinal velocity due to spontaneous emissions. The velocity increment lost is equal to 2R times their initial normal velocity, i.e.,

$$\delta v_x = -2Rv\sin\phi \qquad (8)$$

This effect can be used to enhance the low velocity portion of a thermal beam, by using grazing incidence from an

interface. The population increase due to the downward shifting of velocities from a thermal beam is shown in Figure 4. The result is a 22% increase in the low velocity population under nominal conditions.

In general, for laser illumination at an angle γ from the atomic beam direction (measured in the plane of the interface), the velocity increment will be

$$\delta v_x = 2Rv\cos\gamma\sin\phi \qquad (9)$$

The cases of most interest, however, are counter-propagation ($\gamma = 180^o$) for beam deceleration, co-propagation ($\gamma = 0$) for acceleration, and cross propagation ($\gamma = 90^o$) for transverse deflection. Other angles will yield a combination of acceleration and deflection. In the beam-conducting pipe and trapping applications, the effects are resolved into longitudinal and transverse components to produce elastic bounces for confinement and longitudinal kicks to accelerate the beam. For the enhanced nozzle application, the angle is unimportant except for practical considerations of laser geometry. This is due to the suppression of the kick for this application.

Quantum Considerations. One effect which has been overlooked thus far is a velocity spreading due to the nature of the force. The kick arises from spontaneous decays of the atoms which occur in random directions. The atom experiences a net kick in the direction of the laser because

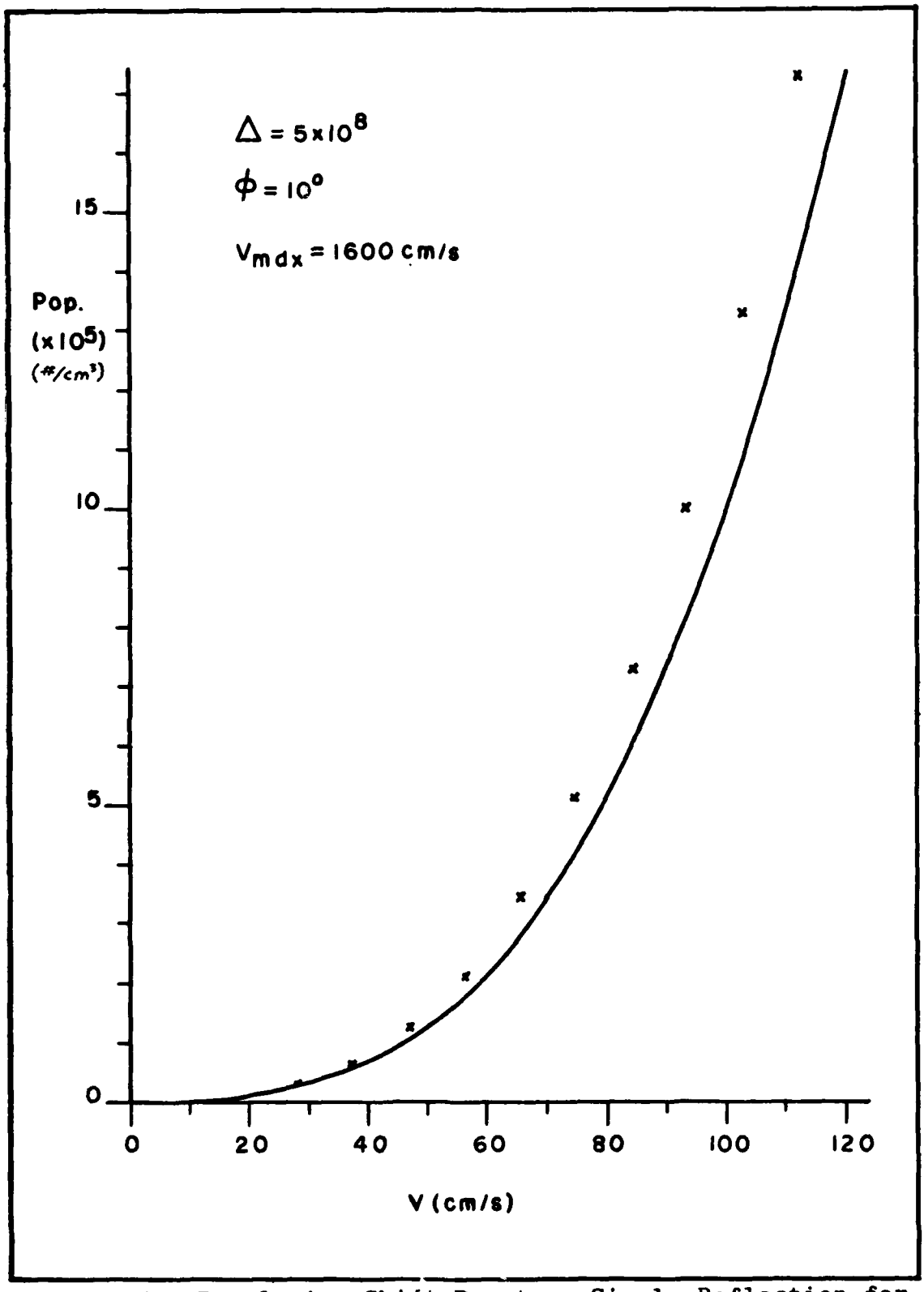

Figure 4. Population Shift Due to a Single Reflection for Sodium Using Moderate Kick

it acquires the momentum of one photon on each absorption. It then loses this momentum in a random direction resulting in an average momentum gain in the direction of the laser's k-vector. The random nature of the emission produces a statistical gaussian spreading of the atom's velocity.

An evaluation of the results of this spreading requires a computation of the numbers involved. On each photon absorption, the atom gains an increment of velocity given by

$$\delta v = \hbar\omega/Mc \tag{10}$$

The number of spontaneous emissions N and the time required for these emissions (essentially the interaction time) δt are then given by

$$N = 2Rv_z Mc/\hbar\omega \tag{11}$$

and

$$\delta t = N/A = 2Rv_z Mc/\hbar\omega A \tag{12}$$

The distribution in velocities is then characterized by σ, the room-mean-square deviation, given by (Ref 26)

$$\sigma = \sqrt{N}\delta v \tag{13}$$

For the two cases of interest, moderate kick and maximum reflection, the velocity increment is the same: $\delta v = 0.47$cm/s per emission. For the moderate kick case and

the limiting normal velocity, N = 320 emissions, $\delta t = 5.2\mu s$, and $\sigma = 8.4cm/s$. For the case of maximum reflection (again at limiting normal velocity), N = 64 emissions, $\delta t = 1\mu s$, and $\sigma = 3.75cm/s$.

This derivation is only approximately correct. A more complete treatment (Ref 14) reveals that the induced spreading is larger than expected. For the mechanism of this thesis, there is an increased spreading in the direction of propagation of the evanescent wave. There is also an induced spread (or diffusion) normal to the surface due to the gradient in the Rabi frequency. A careful analysis of these spreadings was done using the diffusion coefficients obtained by Cook (Ref 14). For the geometry of interest, this required numerical integration of the various diffusion coefficients with respect to time for a path in the evanescent potential well.

The spontaneous root-mean-square deviations vary as the square root of the initial normal velocity of the atom. The induced deviation in the direction of propagation is also proportional to the square root of the initial normal velocity, but is ~25% larger than the spontaneous deviation. The induced deviation normal to the surface is composed of a linear and a cubic term in the initial velocity. Therefore the induced diffusion normal to the surface is much more important at higher atomic velocities! The coefficients for spontaneous and induced diffusion are given in Appendix B

in the BOUNCE routine listing for the two nominal detunings of this thesis. For other detunings, the coefficients should scale roughly as the inverse of the fourth root of the detuning.

Because the induced diffusion normal to the surface varies as the cube of the initial velocity, this term sets an effective upper bound on the initial velocities. For the moderate kick detuning, this induced diffusion is larger than the spontaneous diffusion for velocities above ~70cm/s. For this detuning, the root-mean-square deviation is ~12cm/s for an initial velocity of 100cm/s. For the maximum reflection detuning, the cross-over is at 90cm/s and the deviation at 100cm/s is only 1.8cm/s. For this larger detuning, the deviation does not exceed 10cm/s for initial velocities below 175cm/s.

The deviation in the propagation direction is modest but will tend to enhance the low velocity portion of the beam due to the preponderance of higher velocities in the Maxwell-Boltzmann distribution. The effect on the population is shown in Figure 5 for the moderate kick case. This figure is only an approximation as the integrals involved are analytically unsolvable and numerically unwieldy.

There are two other effects of this gaussian velocity spreading which should be mentioned; spreading of the transverse and normal velocities. The spreading transverse to the atomic beam axis will tend to disperse the beam. This

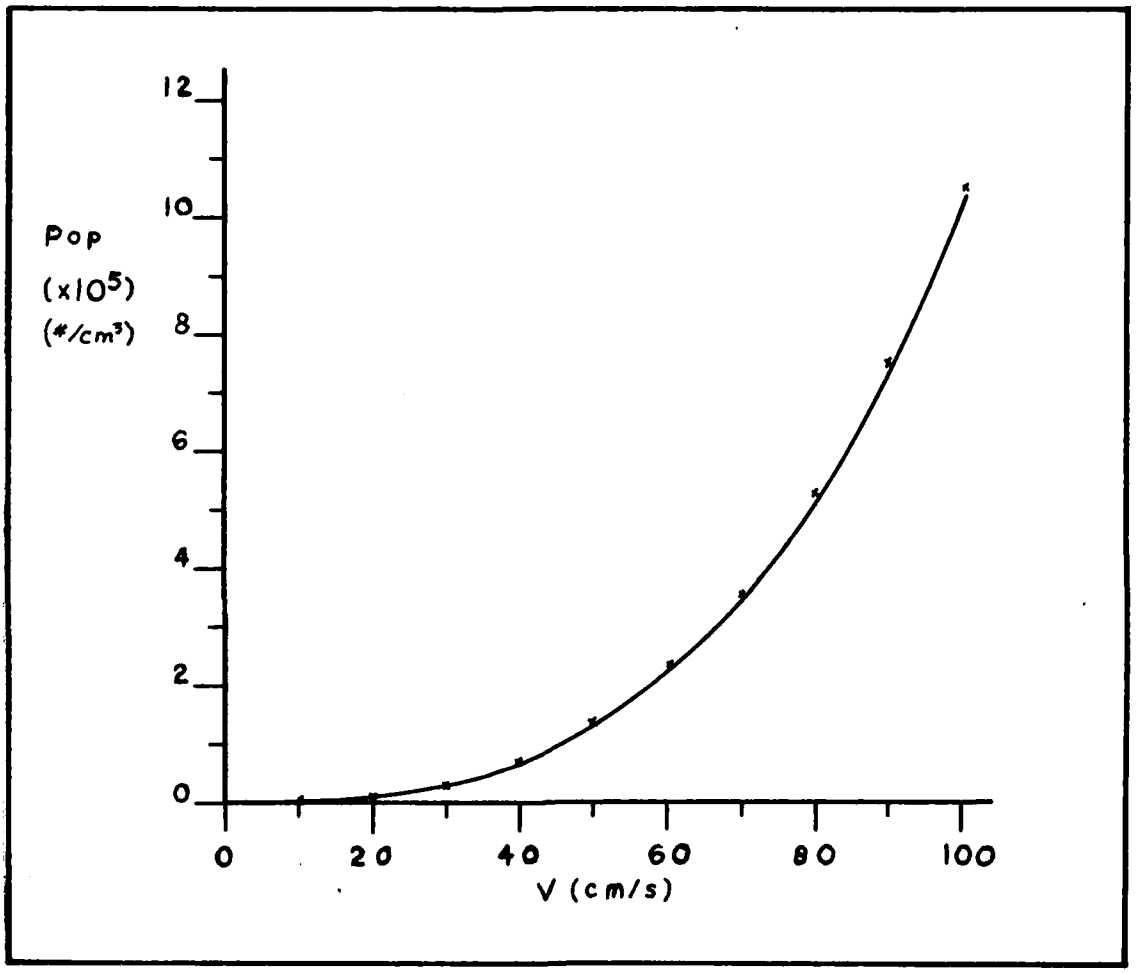

Figure 5. Population Shift Due to Gaussian Spread

dispersion will be small, on the order of inherent dispersions, even for very slow beams. In confinement schemes, it will tend to heat the atoms; but the effect should be minimal. Spreading of the velocity normal to the interface will have two effects. The first effect is the spread of reflected velocities just as in the other directions. The second effect arises from velocity fluctuations during the reflection. Because of these fluctuations, the atom loses the "memory" of its initial normal velocity. This will complicate the reflection process and change the kick and the diffusion in all directions. Fortunately, this effect is very small and will be ignored.

Beam Conducting Pipe

Longitudinal Characteristics. A straightforward extension of the plane mirror in the last section will produce a surface which can be used to conduct a slow atomic beam from one place to another. For this purpose, gravitational trajectories must be considered between interactions. The present section considers only ideal beams of atoms, perfectly collimated, and interacting with the evanescent wave only during an incremental bounce. The first condition will be relaxed to encompass dispersive beams in a later section. The second condition is essentially true for realizable evanescent waves with $n = 1.5$ and $\theta = 45^{o}$.

These give $\alpha = 6 \times 10^3 cm^{-1}$, and the interaction region is on the order of 2 microns deep.

Consider then a horizontal mirror, illuminated as described, and an ideal atomic beam issuing horizontally from a nozzle a distance h above the mirror. The atoms will then fall due to gravity (g) and strike the mirror surface at a distance l given by

$$l = v\sqrt{2h/g} \tag{14}$$

The atoms will be reflected at this point for h such that the normal velocity (due to gravity) is less than υmax as defined earlier. This limits h to

$$h < \upsilon max^2/2g \tag{15}$$

For $\upsilon max \sim 300 cm/s$, this gives a maximum h of ~45cm. This, however, results in excessive values of l. For a maximum $v = 1000 cm/s$ impacting at $l = 1m$, h becomes 5cm. This gives a lower normal velocity and thereby a lesser deceleration on each bounce. A tradeoff must be made based on the initial velocity composition of the beam, the available mirror length, and the purpose of the deceleration. Low velocities are of the most interest for applications in atomic clocks, ultrahigh resolution spectroscopy, etc.

Each atom would be decelerated by the same amount on each bounce:

$$\delta v = 2R\sqrt{2gh} \tag{16}$$

For a mirror of length L, this results in a shift of the initial velocity distribution to lower velocities. Indeed for initial velocities below a cutoff determined by L, the atoms will be retro-reflected toward the nozzle. This shift is illustrated in Figure 6. Note that the shift to lower velocities is incremental. In addition, the atoms are smeared between $z = 0$ and $z = h$ based on the position of the last bounce before they reach the end of the mirror. This vertical distribution, coupled with the incremental nature of the longitudinal velocities at a given height could be used to select a very small velocity segment of the beam.

An interesting result is obtained by solving Eqs (14) and (16) for the time average of the acceleration experienced by an atom. This yields

$$a = (\delta v)v/2l = -Rg \qquad (17)$$

independent of h and v. That is, the reflections act as a simple (but incremental) deceleration of the beam. By tilting the surface (and nozzle) downward this deceleration can be counteracted by gravity to produce an acceleration-free conduction of the atomic beam. The same is true for co-propagation of the laser and an upward tilt of the surface. Because the geometry separates into motion along the surface and a gravitational displacement, the angle of tilt ϕ for acceleration-free conduction is simply

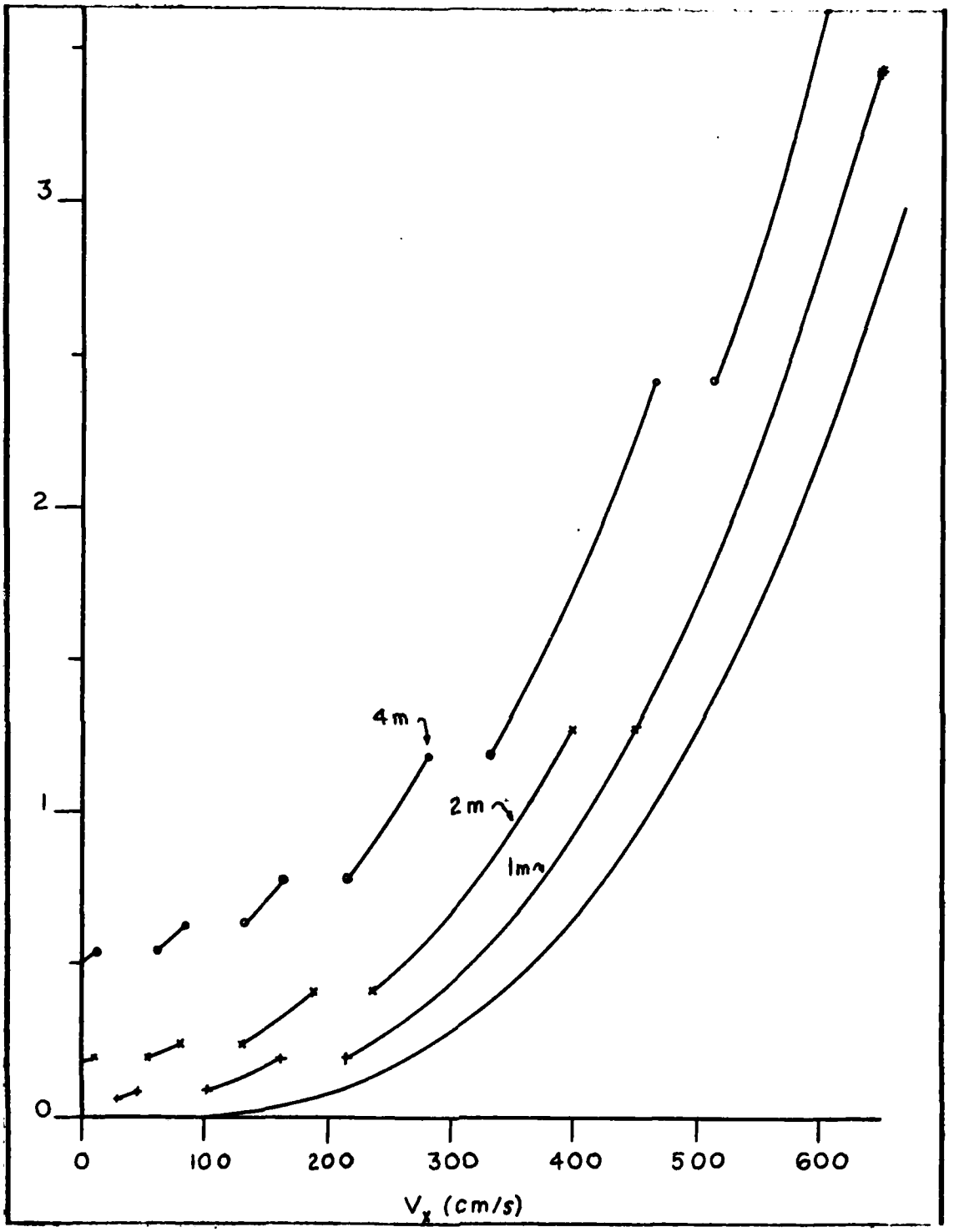

Figure 6. Velocity Shift from Beam Pipe. For each reflection a population group is shifted by ~50cm/s. This results in gaps at some velocities and greatly increased population at others.

$$\phi = \tan^{-1} R \qquad (18)$$

For $n = 1.5$, $\theta = 45^{o}$, and $\Delta = 5 \times 10^{8} s^{-1}$, this yields a tilt angle $\phi = 10.6^{o}$.

By not tilting the surface, the incremental deceleration can be used to increase the low velocity portion of the beam by shifting the more populous segments of the beam to lower velocities. The advantage of this method over deceleration by gravity is the elimination of unwanted velocities at the point of observation (by the incremental vertical shifting), coupled with the transverse confinement of the beam to be discussed in the next section.

Figure 6 shows the dramatic improvement in the low velocity population due to the incremental shift. Although the pipe lengths portrayed were picked for convenience rather than population enhancement, they give rise to significant enhancement. For a pipe length of two meters, the total population of atoms with longitudinal velocities below 100cm/s is increased to over 23 times its original value. For the four meter pipe, the improvement is 35 times the original population. By a proper choice of pipe length coupled with velocity chopping at the output end, a large sample of atoms with very well defined velocity spread can be produced.

The gaussian velocity spread, due to the quantum nature of the force, produces a beneficial result. The

spreading will tend to round the sharp edges of the shifted distributions shown in Figure 6. However, the fact that the initial population is skewed toward the high velocity regime will result in further enhancement of the low velocity portion. The amount of this enhancement is dependent on the pipe length used and no estimate was made.

Transverse Characteristics. Consider now the motion of atoms transverse to the laser direction in the above discussion. Because the induced kick is in the direction of the evanescent wave's k-vector, transverse motion is unaffected except for the gaussian spreading due to the nature of the kick as described above. The effect of this transverse velocity spreading will be ignored for the moment and discussed at the end of this section.

The problem arises as to how the mirror surface can be shaped perpendicular to the atomic beam axis in order to contain and conduct the beam. Because these bounces do not change the transverse speed of the atoms, it becomes a problem in standard kinetics.

For an atom with transverse velocity v_y starting at a height h, its velocity components at any later position (y,z) are given by

$$v_z = \sqrt{2g(h-z)} \tag{19}$$

and

$$v_y = -yg/\sqrt{2g(h-z)} \qquad (20)$$

For retroreflection in the transverse direction, the surface normal must match the velocity vector. This determines z as a function of y for the surface. The result is

$$z = h - \sqrt{h^2 - y^2/2} \qquad (21)$$

a simple ellipse.

This surface will return all atoms to their original apex at $y = 0$ and $z = h$ for transverse velocities up to the maximum limit for reflection. For the moderate kick arrangement (υmax = 289cm/s) and normal collimation (.01 radian) this means that beams chopped for velocities above $2.9x10^4$ can be conducted without loss due to lateral dispersion. This analysis, however, ignores the effect of the vertical component of the dispersion. Simulations using the BASIC program in Appendix B show that the transverse channeling begins to weaken for vertical components at the beam axis in excess of 10cm/s. This weakening is manifested as a shift in the apex position away from $y = 0$. This shift results in a mismatch between the atom's velocity components and the normal vector of the surface. The result is a coupling between the y and z oscillations of the trajectory. The position of the apex shifts after each bounce in an unstable pattern. The observed tendency is toward

higher z values initially, followed by a decay toward lower values. This pattern repeats itself on the order of four bounces.

In order to examine and control this oscillation an attempt was made to design a surface which would compress the lateral motion of the beam. This would effectively focus the beam laterally and greatly enhance the intensity available for subsequent observation. The approach used was a modification of Eq (21) to incorporate a squeezing parameter β. This results in

$$z = h - \sqrt{h^2 - \beta y^2/2} \qquad (22)$$

Results from this approach were disappointing. For $\beta < 1$, the oscillations were intensified. For $\beta > 1$, the oscillations initially reversed, tending toward lower apexes but then continued unabated. These results are included to prevent repetition of these fruitless efforts.

Turning to the gaussian velocity spreading of the beam due to the spontaneous nature of the force, the effect on this transverse confinement scheme is minimal. On each bounce all velocity components will acquire a deviation based on the reflection parameters used.

The result of the spreading of the z component is a spreading of the apex height, and consequent mismatch with the design parameters of the pipe. For a vertical velocity v_z and change in vertical velocity δv, the resultant height

change is given by

$$\delta h = (2v_z \delta v + \delta v^2)/2g \tag{23}$$

The dependence of v_z on v_y is more complicated, but is characterized by

$$v_z = -\sqrt{2gh} + \frac{v_y^2}{4\sqrt{2gh}} - \frac{v_y^4}{32(\sqrt{2gh})^3} + \ldots \tag{24}$$

which leads to a height change of

$$\delta h \approx \delta v^2/2g + .84\sqrt{h}\delta v/g - .84v_y^2 \delta v/\sqrt{h} \tag{25}$$

For the beam pipe parameters described and moderate kick detuning, lateral velocities up to 275cm/s will be reflected. The spreading of the vertical velocities will result in a spread in the apex height on the order of 0.6cm. This is well within the normal spread of heights due to the dispersion of the beam for beam speeds ~700cm/s contemplated in this application.

The spread of velocities in the y direction is somewhat more serious. It results in a transverse shift in the apex position and consequent mismatch with the pipe. Computer simulation has shown, however, that the pipe as described can tolerate transverse velocity shifts on the order of 10cm/s which is roughly the anticipated sigma for 100cm/s transverse velocities. This means that 68% of the

deviations can be handled by the transverse shape of the pipe.

Next, consider the effect of beam dispersion on the use of such a beam pipe. The design is very sensitive to vertical velocity on-axis. This limitation is ~10cm/s, which for collimation of 0.01 radian limits the top beam speed to 10^4cm/s. The lateral requirements are not as severe. The pipe will contain lateral velocities up to 100cm/s with little adverse effect. This can be exploited by using a wide thin opening at the oven coupled with a small opening at the pipe. This gives a fan shaped beam which is vertically narrow. This will result in a 10fold increase in beam intensity over standard collimation, although the output would still contain the lateral velocity spread. However, this will allow placement of detectors in a very pure longitudinal velocity segment of the beam.

One problem which has not been addressed thus far is the matching of the laser radiation to the geometry of the beam conducting pipe. Ignoring the lateral shaping, alignment is simple. The mirror is a flat plane which becomes the top surface of a thin (~1cm) dielectric sheet. The beam output end of the sheet is then given a 45^o bevel and the laser is introduced to the sheet normal to this bevel. When the sheet is curved around the beam axis to provide containment, the situation is not quite so simple.

The inner surface of the pipe is an ellipse, as described earlier. The problem is to find the proper outer shape for the pipe to match the inner curvature. The output end could then be beveled as before, and the laser expanded and focused to strike the normal of the bevel. The radiation would then travel down the pipe much as before, focusing in toward the inner surface, reflecting, expanding toward the outer surface for another reflection, and repeating this process as it traverses the length of the pipe.

The proper shape for the outer surface is another ellipse centered on the beam axis. This ellipse is a distance d larger than the inner surface at all points. The resulting equation is

$$(z-h)^2 = (h+d)^2-x^2(h+d)^2/(\sqrt{2}h+d)^2 \qquad (26)$$

The laser irradiance varies as 1/d, but disturbing waveguide effects occur for d less than ~1mm. Therefore, a determination of the size of d must include consideration of the laser resources available and the user's end purpose for the pipe.

Enhanced Nozzle

One application of resonant reflection which could be of great help in the study of slow atoms is a reflective nozzle to aid beam collimation. Because of the extremely

low populations of slow atoms in a thermal beam, any improvement in collimation without concomitant losses would greatly increase the number of atoms for study.

By forming a parabolic reflector around the beam with a suitable dielectric, such a nozzle can be constructed. The arrangement is shown in Figure 7.

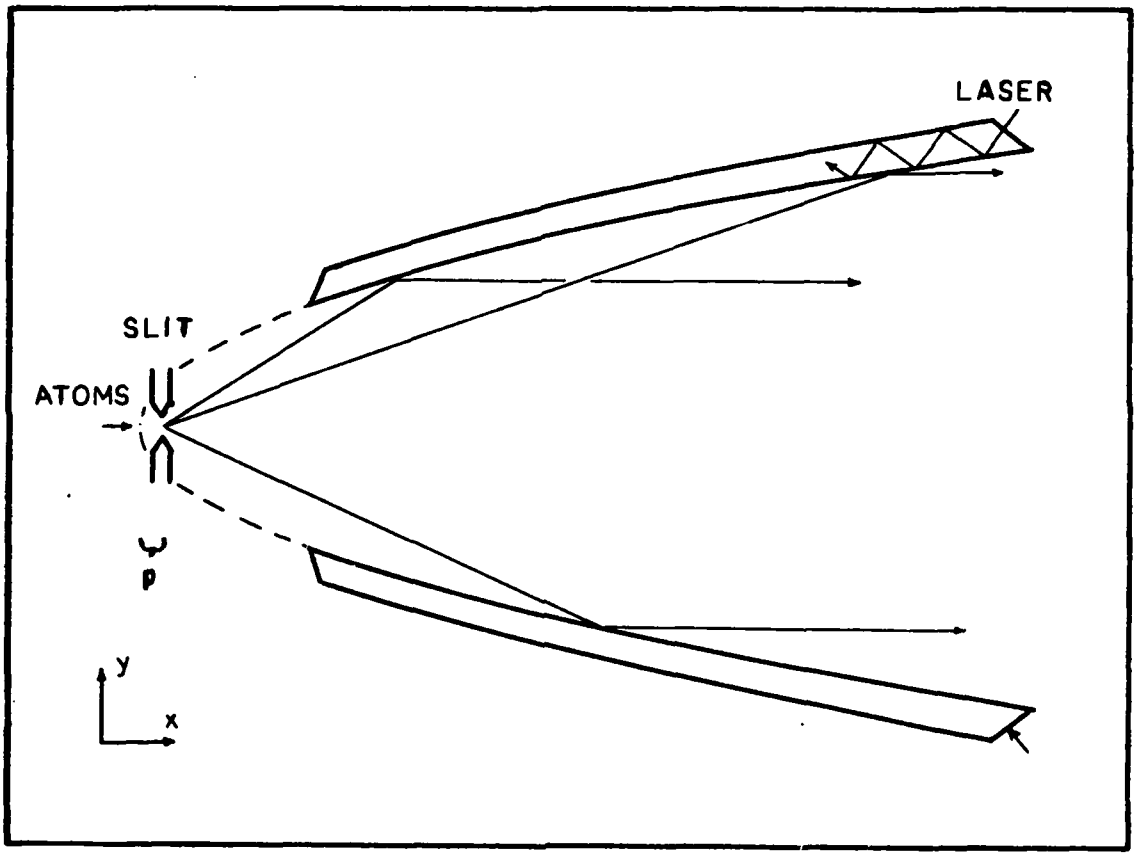

Figure 7. Nozzle Geometry. A beam of atoms diverges from the slit and is reflected from a dielectric paraboloid illuminated from within.

For this application, the induced kick on each bounce is a hindrance. Therefore, use of a large detuning

($5x10^9 s^{-1}$) for maximum reflection and minimum kick is anticipated. This limits the maximum normal velocity at the nozzle surface to 455cm/s. For a small beam source at the focus of the parabola (x=p) [see Figure 7], and atoms issuing at angle θ; the distance to reflection (r), and the x and y coordinates of reflection are given by

$$r = 2p(\cos(\theta)+1/\sin^2(\theta) \quad (27)$$

$$x = p + r\cos(\theta) \quad (28)$$

$$y = r\sin(\theta) \quad (29)$$

At angle θ, the maximum longitudinal velocity which can be reflected is given by

$$v_x^{max} = 455/\tan(\theta)\sin(\theta/2) \quad (30)$$

Thus x velocities up to 3000cm/s can be reflected for angles up to 30^o.

In any application of this resonant nozzle a trade-off must be made between the maximum longitudinal velocity and the maximum angle, and between the length of the nozzle and the minimum angle. To explore the utility of the nozzle, nominal values of 8 and 30 degrees were chosen for the minimum and maximum angles with p = 0.1cm .

These parameters give a maximum longitudinal velocity of 3000cm/s as described above, a nozzle length of 20.5cm and an output radius of 2.9cm. This radius is an order of

magnitude less than that for a collimated beam of 3000cm/s atoms at 1m. In addition, the major portion of the atoms are reflected from the larger angles (where the radial displacement is the least). For angles above 20 degrees, y is less than 1.1cm. At the output end of the nozzle, ignoring the induced kick which will be discussed later, the atoms are perfectly collimated and ready for observation or conduction via a beam pipe for deceleration, etc. The most startling change in the beam is the enhancement of the population available for further manipulation. By collecting and collimating the atoms at angles between 8 and 30 degrees, the number available is 2484 times that contained in the normal .01 radian sample! By using an elliptic (rather than parabolic) nozzle, the input beam can be focused onto a small spot for filling an atomic trap or further manipulation and detection.

Note that gravitational displacement has not been mentioned in the above discussion. This is due to the anticipated velocity range used in this application. For a longitudinal velocity of 700cm/s, the atom will only drop 0.42cm in the 20.5cm length of the nozzle. The drop for higher velocities trails off as the inverse square of the velocity. This effect will be negligible when compared with the focusing effects of the nozzle and the quantum fluctuations due to the nature of the force. The requirement for moderate initial velocities can be negated by using a beam

pipe for deceleration at the output end of the nozzle. Changes in the nozzle parameters will also reduce the gravitational effect. By increasing the minimum angle to 10 degrees, the nozzle length is decreased to 13.1cm from 20.5 with reduction of the population multiplier to 2375 from 2484. It appears that a more serious limitation is the proper construction and alignment of the nozzle and the beam origin.

Returning to the kick induced on the bounce, there are three effects worthy of note. Assuming counter propagation of the laser, these are a deceleration of the atoms, an over-focusing due to the angle of reflection, and the inevitable qaussian velocity spreading in all directions.

The deceleration is given by

$$\delta v_x = 2Rv_x \tan\theta \sin(\theta/2)\cos(\theta/2) \qquad (31)$$

For the parameters above, this is a fairly modest effect. For v_x = 3000cm/s and $\theta=30^o$, the deceleration is only 16cm/s, decreasing rapidly for lower velocities and angles.

The kick also has a component in the radial direction. This serves to increase the focusing effect of the parabola, and is given by

$$\delta v_f = 2Rv_x \tan\theta \sin^2(\theta/2) \qquad (32)$$

For the nominal parameters above, this is never more than 4.4cm/s, and is typically less than 1cm/s. This is well

within the allowable range of deviations and less than the effect of the gaussian velocity spread.

The effect of the gaussian velocity spread can be resolved into three components. For the maximum kick detuning used in this application, the spread is characterized by a root-mean-square deviation of 10cm/s times the cube of the ratio of the normal velocity over 175cm/s. The spread in the axial direction can be ignored relative to the axial velocities ranging in the thousands. There is, of course, the beneficial effect on the lower velocity portion due to the skewed initial population. The spreading of velocities in the ϕ direction can also be ignored as it is negligible compared to construction and misalignment effects. The radial component of the spreading is alone worthy of further examination.

The radial spreading component is the major innate cause of defocusing, second only to misalignment of the beam source. The effect is only significant for longitudinal velocities above ~750cm/s. For this longitudinal velocity, the radial velocity induced at two sigma (which encompasses 95% of the deviations) is only 7.5cm/s, within allowable limits for a subsequent beam pipe and corresponding to a 0.1 radian collimation at 750cm/s.

The problem of laser illumination is more serious. The nozzle should be formed with a parabolic interior, and an outer shape which ensures a constant angle between the

laser, multiply reflecting down the dielectric interior, and the interior interface. The equation for the outer shape unfortunately involves an integral with no analytic solution. In fact, there is no outer shape which will satisy the requirement exactly. The best solution is a thin-walled paraboloid which will allow very little variation in the interface angle over the length of the pipe. As long as the wall is thick enough to avoid spill over problems associated with thin waveguides, the variation should not be significant. One factor working in the designer's favor is the inherent narrowing of the paraboloid. This insures that the effective illumination will be more intense near the base of the paraboloid due to the smaller effective area. This will help compensate for the varying angles of incidence. For the parameters above and a 0.25cm thick wall, no insurmountable problems are foreseen.

Trap for Slow Atoms

The lateral confinement scheme used in the beam conducting pipe is the starting point for a scheme to trap and hold slow atoms for observation. The system is already bound in four directions: plus z by gravity, minus z by the reflecting surface, and plus and minus y by the elliptical walls of the cavity. The remaining problems are in overcoming the induced kick, designing the x variation of the trap, evaluating the effectiveness and usefulness of the

trap, and finding methods for laser illumination and atom introduction into the trap.

Overcoming, or at least reducing, the induced kick is the easiest part of this problem. By using a detuning for maximum reflection, the kick is reduced by an order of magnitude from its value when detuning for a moderate kick is used. Three other factors are introduced by using the higher detuning. First, the maximum normal velocity is raised, deepening the trap. Second, the length of time of the interaction is reduced by an order of magnitude due to the increased potential. This reduces the chances of an unwanted atomic transition out of resonance, and thereby improves the overall efficiency of the reflection. Finally, the gaussian spread of velocities is reduced by the use of a higher detuning. This follows from the Quantum Considerations section of the Basic Mechanism discussion.

Design of the x variation of the trap is more difficult. The obvious solution is to extend the lateral shape to the longitudinal direction. This will result in an elliptic cup which would return all atoms to their original apex position. The problem with this approach originates in the inherent kick. To preserve the lateral confinement the laser radiation must be directed along the x axis. This produces a kick in the x direction. For an anticipated size of the trap on the order of $h = 10cm$, the normal velocity due to gravity is 140cm/s on axis. This produces a kick of

5.2cm/s on each bounce. This is larger than the sigma for the velocity spread (1.8cm/s), but the problem is really in the consistency of direction for multiple bounces. The velocity increments due to the kick are additive, leading to an acceleration out of the trap, whereas the gaussian spreading results in no net acceleration.

Two alternative approaches present themselves for solution of this net acceleration. The first is to switch the direction of the laser on a time interval which will catch the atoms on alternate bounces. This would be tricky and wasteful of laser resources. In addition, the atoms have a different time between bounces dependent on their velocity perpendicular to the laser axis. Finally, this approach has the drawback of losing atoms which strike the surface during the laser direction switch. This will quickly lead to depletion of the trapped population and, more importantly, damage to the surface and consequent degradation of the reflection and trapping. The second approach is to tilt the x variation of the elliptical cup to allow gravity to counteract the inherent acceleration. This approach will be examined in detail.

The addition of a tilt to the ellipse for longitudinal trapping involves the addition of an extra term in the differential equation defining the surface. The equation becomes

$$\frac{dz}{dx} = \frac{v_z}{v_x} + R \tag{33}$$

Unfortunately, this results in a nonlinear equation which defies analytic solution. Because R is a small parameter in the proposed application, perturbation theory was used to obtain an approximate form for the longitudinal shape. The equation can be written (to an error on the order of $R x^2/4h^2$) as

$$z = Rx + \frac{x^2}{4h} + \frac{Rx^3}{4h^2} + \frac{(8R^2+1)x^4}{32h^3} \tag{34}$$

The purpose of the shape change is to absorb the additional momentum of the kick and to redirect it in the z direction. This results in an incremental raising of the apex position with no change in the longitudinal position.

The effect of the gaussian spread is to shift the position of the trajectory apex. This causes a misalignment of the trajectory with the design parameters of the trap. This will not normally lead to escape from the trap, but results in a spread in the population available for observation at the apex position. The position spread depends in a complicated manner on the initial velocity components of the atom, and how long it stays in the trap. The effect of a misalignment tends to be carried through subsequent bounces and is slightly enhanced rather than mitigated. Repeated

simulations have shown, however, that the variation is on the order of 1cm for the trap parameters given after ten bounces, which takes 2.5sec.

The reliable position of the atomic apex on time scales measured in seconds is at the crux of this trap design. For a trap scale of $h = 10cm$, the atoms will be at the apex at ~0.27 second intervals. They will fall 1cm in 0.045 seconds. Therefore, fully one third of the time an atom is trapped, it is in the top 10% of the trap with vertical velocity below 45cm/s. Equipment can then be trained on the apex position to use slow atoms in free flight, without laser interactions and with a very small spread of velocities.

Laser illumination of the trap is somewhat tricky. At the interior interface, the radiation must be aligned in the x direction. This is topologically impossible. The nearest realizable alternative is to reflect the radiation along the interior of the trap in a meridian flow. That is to illuminate the trap at one end ($y = 0$) with an expanding wavefront. Ignoring the tilt correction, if the focus of the laser is at $(\sqrt{2}h,0,h)$ the radiation will follow the curve of the bowl around to $(-\sqrt{2}h,0,h)$. These paths result from using a constant thickness of dielectric for the trap and ignore the gaussian propagation anomalies of the laser beam. This oversight can be mitigated by cutting a small semi-circle out of the dielectric around the laser focus and

beveling this edge for normal incidence. The correction to this procedure necessitated by the longitudinal tilt is straightforward. The radiation will still follow the meridians of the tilted bowl.

There are two further problems with the above arrangement. The first is the requirement for large laser intensities. At the center ellipse of the trap (x = 0) the length of the ellipse is approximately $h\pi\sqrt{3/2}$. For h = 10cm , this gives ~38.5cm. For dielectric thickness d, the laser covers a longitudinal length 2d on each reflection. Therefore, the laser illumination is spread over an area ~77d cm^2. With a thickness of 2mm and laser intensity of 1watt, a sufficient electric field can be generated. Smaller values of d will result in unwanted waveguide effects. The second problem involves the placement of observation equipment. This can be accommodated by restricting the size of the trap lateral to the laser propagation. By removing two sections from the top of the trap (10 degrees meridionally), sufficient room is provided for horizontal observation of the apex region without significant loss to the trapping potential of the device. This has the advantage of reducing the laser power required, though only slightly.

The introduction of the atoms into the trap is another problem which should be addressed. The atoms can enter the trap through a small hole (~1mm), low on the side of the trap. If they have approximately the right velocity

and are sufficiently collimated they will then bounce freely in the trap until they spontaneously shift out of resonance or pick up sufficient horizontal velocity to escape. Simulation has shown that the spread in apex position makes the atoms unsuitable for observation after 10 to 20 bounces. This should be before either of the other effects removes them from the trap. Each atom has an effective observation time on the order of one second spread over a lifetime of three seconds.

The requirements on the collimation and velocity of the injected atoms are stringent. However, the beam nozzle of the preceding section and deceleration by a suitable beam pipe are ideally suited to provide a large number of suitably prepared atoms.

III. Analysis and Conclusions

General Considerations

An analysis of evanescent resonant reflection and three possible applications has been presented in the preceding sections. The analysis has focused on the production and manipulation of very well collimated and very slow (~100cm/s) beams of neutral particles. The questions which should be asked of the applications presented are as follows. First, are the proposed applications feasible using existing technology? Secondly, are the applications useful in the study of neutral particle phenomena? And finally, are these applications more effective than existing and proposed methods for the manipulation of atomic beams? These are the considerations which should be addressed in an evaluation of these results.

Criteria for Evaluation

In assessing the answers to the three considerations of the previous section, quantifiable criteria should be adopted. This section attempts to define such criteria.

The question of feasibility involves a knowledge of current technology in tunable laser power. In addition, the manufacture of precise dielectric surfaces and the focusing of the available laser power must be considered. Finally, the current state of neutral beam production should be

addressed as it relates to the input parameters for any of the proposed application. Available technology is the best guarantor of feasibility.

Current tunable laser power technology is available from a literature search. Powers of one watt are common in the literature of sodium experiments (Refs 4-7). One of the largest power levels found was 40kW (pulsed) for a tunable dye laser (Ref 32). The nominal one watt power level used in assessing the applications in this thesis is easily attainable.

The ability to manufacture precise dielectric surfaces does not appear to be a problem. Current lens manufacturing techniques can be used to form the necessary shapes. Focusing the laser power onto the interface is likewise well understood. The major problems are waveguide and diffraction effects which are combatted by using thicker dielectric slabs or more laser power.

Neutral beam production is the current weak link in the study of neutral atom characteristics. Atomic ovens produce a large flux of atoms into a 2π solid angle. The problem is that baffles must currently be used to effect collimation. Beam collimations from .01 to .0005 radian are used in beam experiments (Ref 18). These equate to 5×10^{-5} to 1.25×10^{-7} of the atoms issuing from the oven. This means that months are required to observe the equivalent of minutes of oven output.

The usefulness of applications must be based on the end uses for the atomic beams. The major uses are collision and deflection experiments with very well collimated beams, and atomic spectroscopy with slow beams or trapped atoms. In either case, the criteria reduce to the spread of velocities. For beam collimation, lateral velocity is most important. For trapping, all components of velocity are considered.

The effectiveness of beam control techniques must be judged on the final velocity spread and the required laser power and oven production. This is the final criterion for beam control applications.

Comparison With Existing Results

Deflection. The deflection of neutral beams was made possible only recently by the use of resonance-radiation pressure (Refs 1-3; 18; 22). The spontaneous force was used by Scheider et al. (Ref 18) to deflect a beam, but only marginal success was achieved (~28cm/s). Cook and Bernhardt proposed (Ref 22) and Arimondo et al. confirmed (Ref 3) the possibility of using the induced transition rate for deflection. This results in a statistical variation with Ωt as the driving variable. Deflections from a standing wave pattern using this scenario can be very high. The tangent of the deflection angle varies as $1/v^2$. For initial velocities of $<10^6$cm/s the deflection is greater than 1^o.

Using the electromagnetic mirror of this thesis, a 1^{o} deflection can be achieved for beam velocities below 52000cm/s (using detuning for maximum reflection and one watt power). Therefore, the evanescent effect is 20 times weaker than a standing wave deflection. The advantage of the evanescent reflection is its sharply controllable position and orientation.

Focusing. The controllability of evanescent reflection is most evident in the focusing of a diverging atomic stream.

The current method of focusing a neutral atomic beam is to co-propagate a gaussian laser beam tuned below the resonant transition. This causes a dipole force on the atoms which deflects them toward the center of the laser beam (the most intense position). This focusing effect has been observed by Bjorkholm et al. (Ref 5). They report that the atomic trajectories are sinusoidal at a frequency of ~4kHz with transverse confinement for radial velocities below 190cm/s.

There are two objections to this method of focusing. The first is that the beam can only be confined along the straight path of the laser. For most applications this is only a minor hindrance. The second objection is that the sinusoidal trajectories provide good containment but limited focusing or collimation. Ignoring the gaussian velocity spread, the radial velocity of a contained atom is less than

10% of its maximum value for 6% of its trajectory. The radial velocity is within 10% of its maximum value for 29% of the time.

The enhanced nozzle of this thesis, in contrast, redirects the radial components of a divergent atomic beam. The effect, again ignoring the gaussian velocity spread, is to produce a perfectly collimated beam. For other applications, the paraboloid can be reshaped into an ellipsoid. This will focus a large portion of the beam onto a small spot. No comparable effect has been reported in the study of vacuum resonant radiation pressure.

Trapping. The current literature contains many proposals for atomic traps. The most promising design is that of A. Ashkin, first outlined in 1978 (Ref 10). This design appears capable of trapping and cooling atoms whose initial velocity components are less than 500cm/s radially and $2x10^4$cm/s axially. An important measure of trap performance is the Boltzmann factor: the ratio of confining potential well depth to the minimum energy attainable. Ashkin calculates a Boltzmann factor of ~100 for his trap. This compares favorably to the Boltzmann factor of ~1 for other trapping proposals.

The trap described in this thesis has a Boltzmann factor of ~2-10 depending on the design size and the introduction conditions placed on the atoms. The major advantage of this trap over all others in the literature is the

illumination-free observation of the atoms. The trap has a slightly longer containment time, a ten thousand fold increase in the laser-free observation time, and more stable atomic velocities than the Ashkin trap. When used in conjunction with an enhanced nozzle and beam pipe deceleration, either trap can enjoy a greatly enhanced trapping rate.

Conclusions

The phenomena of evanescent resonant reflection is worthy of further theoretical study and experimental verification. The unique properties of this phenomena show great initial promise in the field of neutral beam control. There are distinct possibilities in the areas of controlled deflection, atomic trapping, and particularly in the collimation and focusing of divergent beams.

Further theoretical study should concentrate on the strength of induced diffusion normal to the reflecting surface and the identification of additional promising geometries and applications. The induced diffusion is still the major limiting factor on the applicability of this technique. For the parameters of this thesis, the induced diffusion precludes specular atomic reflection for normal velocities above ~400cm/s.

Experimental verification of the essential features of the effect is also needed. The magnitude of the forces

and diffusion coefficients involved can be verified by conducting fairly simple deflection experiments. The construction and testing of a beam pipe should also yield results which would confirm (or deny) the analysis presented.

Bibliography

1. Bernhardt, A. F., et al. "Separation of Isotopes by Laser Deflection of an Atomic Beam. I. Barium," Applied Physics Letters, 25: 617-620 (1974).

2. Bernhardt, A. F. "Isotope Separation by Laser Deflection of an Atomic Beam," Applied Physics, 9: 19-34 (1976).

3. Arimondo, A., H. Lew and T. Oka. "Deflection of a Na Beam by Resonant Standing-Wave Radiation," Physical Review Letters, 43: 753-757 (1979).

4. Bjorkholm, J. E., A. Ashkin and D. B. Pearson. "Observation of Resonance Radiation Pressure on an Atomic Vapor," Applied Physics Letters, 27: 534-537 (1975).

5. Bjorkholm, J. E., et al. "Observation of Focusing of Neutral Atoms by the Dipole Forces of Resonant-Radiation Pressure," Physical Review Letters, 41: 1361-1364 (1978).

6. Balykin, V. I., V. S. Letokhov and V. I. Mishkin. "Cooling of Sodium Atoms by Resonant Laser Emission," Soviet Physics JETP, 51: 692-696 (1980).

7. Phillips, W. D. and H. Metcalf. "Laser Deceleration of an Atomic Beam," unpublished article. Center for Absolute Physical Quantities, National Bureau of Standards, Washington, D. C.

8. Ashkin, A. "Applications of Laser Radiation Pressure," Science, 210: 1081-1088 (1980).

9. Ashkin, A. "Acceleration and Trapping of Particles by Radiation Pressure," Physical Review Letters, 24: 156-159 (1970).

10. Ashkin, A. "Trapping of Atoms by Resonance Radiation Pressure," Physical Review Letters, 40: 729-732 (1978).

11. Letokhov, V. S. and V. G. Minogin. "Trapping and Storage of Atoms in a Laser Field," Applied Physics, 17: 99-103 (1978).

12. Ashkin, A. and J. P. Gordon. "Cooling and Trapping of Atoms by Resonance Radiation Pressure," Optics Letters, 4: 161-163 (1979).

13. Gordon, J. P. and A. Ashkin. "Motion of Atoms in a Radiation Trap," Physical Review A, 21: 1606-1617 (1980).

14. Cook, R. J. "Theory of Resonance-Radiation Pressure," Physical Review A, 22: 1078-1098 (1980).

15. Einstein, A. "On the Quanta Theory of Radiation," Zeitschrift für Physik, 18: 121-128 (1917).

16. Frish, R. "Experimental Detection of the Einstein Recoil Radiation," Zeitschrift für Physik, 86: 42-48 (1933).

17. Ashkin, A. "Atomic Beam Deflection by Resonance-Radiation Pressure," Physical Review Letters, 25: 1321-1324 (1970).

18. Schieder, R., H. Walter and L. Wöste. "Atomic Beam Deflection by the Light of a Tunable Dye Laser," Optics Communications, 5: 337-340 (1972).

19. Kazantsev, A. P. "Acceleration of Atoms by a Resonance Field," Soviet Physics JETP, 36: 861-864 (1973).

20. Hänsch, T. W. and A. L. Schawlow. "Cooling of Gases by Laser Radiation," Optics Communications, 13: 68-69 (1975).

21. Kazantsev, A. P. "Resonance Light Pressure," Soviet Physics USP, 21: 58-76 (1978).

22. Cook, R. J. and A. F. Bernhardt. "Deflection of Atoms by a Resonant Standing Electromagnetic Wave," Physical Review A, 18: 2533-2537 (1978).

23. Cook, R. J. "Theory of Atomic Motion in a Resonant Electromagnetic Wave," Physical Review Letters, 41: 1788-1791 (1978).

24. Cook, R. J. "Atomic Motion in Resonant Fluctuating Laser Radiation," Physical Review A, 21: 268-273 (1980).

25. Allen, L. and J. H. Eberly. Optical Resonance and Two-Level Atoms. New York: John Wiley and Sons, Inc., 1975.

26. Reif, S. Statistical Physics. New York: McGraw Hill, 1967.

27. Bernhardt, A. F. "Isotope Separation by Laser Deflection of an Atomic Beam," Applied Physics, 9: 19-34 (1976).

28. Stenholm, S. "Theoretical Foundations of Laser Spectroscopy," Physics Reports, 43: 151-221 (1978).

29. Jackson, J. D. Classical Electrodynamics. New York: John Wiley and Sons, Inc., 1962.

30. Cook, R. J. "Atomic Motion in Resonant Radiation: An Application of Ehrenfest's Theorum," Physical Review A, 20: 224-228 (1979).

31. Cook, R. J. "Quantum-Mechanical Fluctuations of the Resonance-Radiation Force," Physical Review Letters, 44: 976-979 (1980).

32. "Cylindrical Frequency Doubler Shows Broad Tuning Range," Laser Focus: 18-20 (August 1982).

Appendix A

Optics Communication Article

The genesis of this thesis was an idea by Dr. Richard Cook of the AFIT staff. This idea is expressed and expounded in the following article accepted for publication in Optics Communications. The article outlines the use of evanescent waves for the manipulation of beams of neutral atoms. The quantum mechanical basis for the force laws is reviewed, and conjectures are made as to possible applications. The author of this thesis is included as a co-author of the article because of efforts in verifying the derivation and assessing the implications for neutral beam control.

The article is presented as written, with only necessary modifications to the form, bibliography, and citation. The salient features of the article are also presented in the Basic Mechanism portion of section II of this thesis. Note the citations are to the bibliography on page 52 while the equations are numbered as they appear in the journal article.

AN ELECTROMAGNETIC MIRROR FOR NEUTRAL ATOMS

Richard J. Cook
Richard K. Hill

Abstract

When light is totally reflected internally at a vacuum-dielectric interface, an atom in the thin transmitted evanescent wave experiences a radiation force. For light tuned above the transition frequency of a two-level atom, this force tends to repel the atom from the dielectric surface; and hence the internally illuminated surface acts as a mirror for slow neutral atoms. This paper presents the first analysis of this atomic reflection process and suggests that the effect can be used to trap slow atoms or to focus a slow atomic beam.

In recent years, a number of techniques have been proposed for controlling the motion of atoms or molecules by means of the radiation force of laser light propagating freely in vacuum [5; 9-13; 17; 20-23; 27; 28]. This paper describes a new scheme for controlling atomic motion which makes use of the radiation force exerted by the thin evanescent wave that is generated on the surface of a dielectric medium when laser light is totally reflected internally at that surface. Specifically, we show that, when the light is tuned above an atomic resonant frequency, a slow atom is reflected by the evanescent wave without making contact with the material surface.

If a plane electromagnetic wave of frequency ω propagates in a medium of refractive index n and is totally reflected internally as depicted in Figure 8, then the electric field of the transmitted evanescent wave takes the form [29]

$$\vec{E}(\vec{x},t) = \hat{\varepsilon}\xi e^{-\alpha y}\cos(\omega t - kx) \qquad (1)$$

where $\hat{\varepsilon}$ is a unit polarization vector,

$$\alpha = \omega(n^2\sin^2\theta - 1)^{\frac{1}{2}}/c, \qquad (2)$$

$$k = \omega n\sin\theta/c \qquad (3)$$

θ is the angle of incidence of the wave, and ξ is the wave amplitude at $y = 0$. The condition for total internal reflection is $\theta < \theta_c = \sin^{-1}(1/n)$. The evanescent wave

propagates parallel to the dielectric surface and is substantial only within a few wavelengths of the surface, except for $\theta \approx \theta_c$.

Now an atom in the evanescent wave experiences a radiation force due to momentum transfer from the wave. For a two-level atom with transition frequency ω_o and a near-resonant field ($\omega \approx \omega_o$), the radiation force has a component [30]

$$F_y = \frac{2\alpha\hbar(\Delta-kv_x)\Omega^2(y)}{4(\Delta-kv_x)^2+A^2+2\Omega^2(y)} \qquad (4)$$

normal to the dielectric surface associated with the gradient of the field amplitude (the dipole force), and a component

$$F_x = \frac{\hbar kA\Omega^2(y)}{4(\Delta-kv_x)^2+A^2+2\Omega^2(y)} \qquad (5)$$

parallel to the surface (the spontaneous force), where $\Delta = \omega-\omega_o$ is the detuning frequency, v_x is the x-component of the atomic velocity, $A = 4\mu^2\omega_o^3/3\hbar c$ is the Einstein spontaneous emission coefficient, and $\Omega(y) = \mu\xi\exp(-\alpha y)/\hbar$ is the on-resonance Rabi frequency of the two-level atom (μ is the dipole transition moment). Equations (4) and (5) are valid when the Rabi frequency $\Omega(y)$ and the Doppler shift kv_x are slowly varying functions of time on the time scale of the atomic relaxation time $\tau = 1/A$ [30]. For simplicity, the following discussion is limited to the case in which the

detuning Δ is positive ($\omega > \omega_o$) and is large compared to the Doppler shift kv_x. Then, to a good approximation, Eqs (4) and (5) reduce to

$$F_y = \frac{2\alpha\hbar\Delta\Omega^2(y)}{4\Delta^2+A^2+2\Omega^2(y)} \tag{6}$$

$$F_x = \frac{\hbar k\Delta\Omega^2(y)}{4\Delta^2+A^2+2\Omega^2(y)} \tag{7}$$

Because $\Delta>0$, F_y tends to repel the atom from the dielectric surface. The normal force F_y, taken alone, is derivable from the potential energy

$$V(y) = (1/2)\hbar\Delta\ln[1+2\Omega^2(y)/4\Delta^2+A^2)] \tag{8}$$

Therefore, an atom of mass M initially moving toward the surface with velocity v_y is reflected by the thin evanescent wave if $\frac{1}{2}Mv_y^2 < V(0)$, i.e., the maximum reflected velocity is

$$v_y^{max} = \{\frac{\hbar\Delta}{M}\ln[1+\frac{2\mu^2\xi^2}{\hbar^2(4\Delta^2+A^2)}]\}^{\frac{1}{2}} \tag{9}$$

Next we derive the law of reflection for the atomic trajectory. From Eqs (6) and (7) the ratio of the tangential to the normal force is seen to be

$$R = \frac{F_x}{F_y} = \frac{kA}{2\alpha\Delta} = \frac{nA\sin\theta}{2\Delta(n^2\sin^2\theta-1)^{\frac{1}{2}}} \tag{10}$$

This ratio is independent of position. Therefore, the increments of velocity, Δv_x and Δv_y, experienced by the atom during the reflection process must have the same ratio ($\Delta v_x = R\Delta v_y$), and since in reflection $\Delta v_y = -2v_y$, where v_y is the initial (negative) normal velocity, we have $\Delta v_x = -2Rv_y$. Suppose now that the atom moves in the xy plane as illustrated in the Figure. Then from the geometry of the initial and final velocity vectors, it is easy to show that the atomic trajectory obeys the law of reflection

$$\tan\phi_r = \tan\phi_i - 2R \qquad (11)$$

where the angle of incidence ϕ_i and the angle of reflection ϕ_r are algebraic quantities measured in the sense indicated in Figure 1. Note that a positive ϕ_i indicates that v_x is initially opposite to the propagation direction of the evanescent wave. Equation (11) has the solution $\phi_r = -\phi_i$ for $\phi_i = \tan^{-1}R$. For this angle of incidence, the atom is retroreflected. When R is negligibly small (R<<1), Eq (11) reduces to the simple reflection law $\phi_r = \phi_i$. According to Eq (10), this occurs when the detuning Δ is much larger than the Einstein A-coefficient, except for $\theta \sim \theta_c = \sin^{-1}(1/n)$. It should be noted that if the atom has a component of velocity in the z-direction, the planes of incidence and reflection of the atomic trajectory are not, in general, the same because of the impulse delivered to the atom in the x-direction. However, as R→0 these planes

become coincident and the simple reflection law $\phi_r = \phi_i$ is again obtained.

To estimate the atomic velocity v_y^{max} that can be reflected in practice, we suppose that a z-polarized electromagnetic wave of intensity I enters the dielectric normally through a plane surface not shown in Figure 8. By a straightforward application of Fresnel's reflection formulas [29], it is found that the square of the evanescent wave amplitude is $\xi^2 = 128\pi n^2\cos^2\theta I/(n^2-1)(n+1)^2/c$. Let the intensity and angle of incidence of the wave by $I = 1$ watt/cm^2 and $\theta = 60^o$, respectively, and let the refractive index of the dielectric be $n = 1.5$. Then for reasonable atomic parameters ($M = 4x10^{-23}g$, $\omega_o = 3x10^{15}s^{-1}$, $A = 10^8s^{-1}$, and detuning $\Delta = 5x10^8s^{-1}$), one obtains from Eq (9) the value $v_y^{max} = 110cm/s$. In a strong field ($\Omega_o = \mu\xi/h >> A$), v_y^{max} assumes its maximum value $v_y^{max} \approx 0.75(h\Omega_o/M)^{\frac{1}{2}}$ for detuning $\Delta \approx 0.56\Omega_o$, and since $\Omega_o \alpha I^{\frac{1}{2}}$, this implies that the upper limit on v_y^{max} is proportional to $I^{\frac{1}{4}}$, which is a rather slowly increasing function of intensity. Therefore, the available tunable CW laser power (~1watt) limits v_y^{max} to values of order 100-400cm/sec for mirror areas ranging from 1cm^2 to 1mm^2. However, values of v_y^{max} approaching typical thermal velocities (~10^4cm/s) can be achieved for very short time intervals by use of pulsed laser radiation.

The above considerations suggest a new type of trap for slow neutral atoms. Suppose that laser radiation is totally reflected by each of the six faces of a cubical cavity in a dielectric medium. Then a slow atom inside the cavity will be reflected by the evanescent waves on the cavity walls without making thermal contact with the dielectric itself. In this way a cold atomic vapor ($T \lesssim 5\times10^{-4}K$) might be held in the cavity for a time sufficiently long to perform essentially Doppler-free spectroscopy. An advantage of this type of trap is that the atoms interact with the radiation only during the brief reflection processes, and consequently the quantum fluctuations of the radiation force [14; 31], which tend to heat the atomic vapor, are much less of a problem than in those schemes in which the atoms are continuously illuminated.

Other possible applications of the reflection process immediately come to mind. For example, it is evident that the dielectric surface in Figure 8 can be given a small curvature to produce a concave mirror for neutral atoms. Such a mirror could be used to focus an atomic beam of slow atoms or to image atoms that are scattered by a small object. Moreover, a complete "optics" of atomic beams could be constructed on the basis of such reflecting elements. But in this connection, it is very important to note that gravity will play an important role, since, for the velocities of

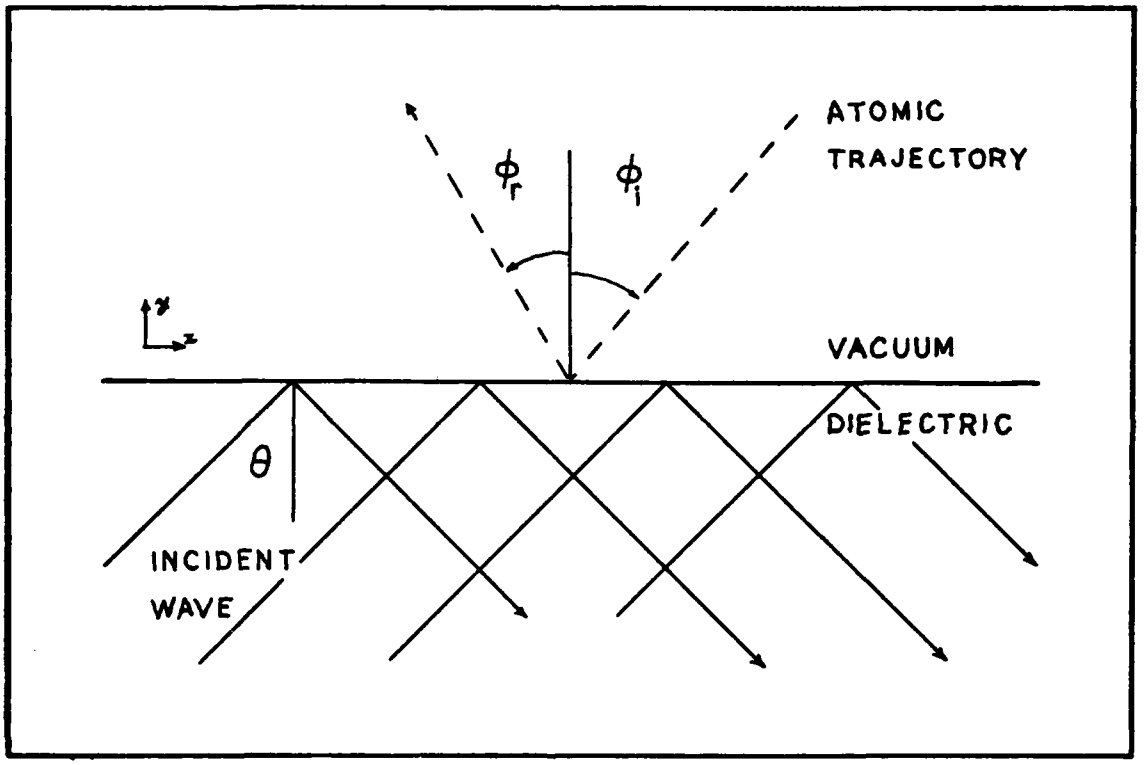

Figure 8. A plane electromagnetic wave is totally reflected internally at the vacuum-dielectric interface. A reflected atomic trajectory, with angle of incidence ϕ_i and angle of reflection ϕ_r, is shown as a dashed line.

interest (~100cm/sec), the atomic trajectories are bent significantly by gravity over a distance of a few centimeters.

Appendix B

BASIC Program

General

In an effort to understand and examine the basic mechanism of resonant reflection, and to test possible applications, the following computer program was written. The language used is BASIC as implemented on an H89 using CP/M. The program was made as flexible as possible and incorporates several user-defined routines.

The user can define any mirror geometry within reason. As listed, the program defines the mirror surface ZSURF as a function of X and Y. Complete three dimensional surfaces are possible with slight modifications, as was used to test the Enhanced Nozzle application. This simply involves the use of in and out, instead of above and below, in the definition of the surface and the intercept location routine. For the sake of execution speed, a separate routine calculates the mirror normal for orientation of the reflection.

Three dimensional laser variations are also definable in the WAVEFRONT routine. The subroutine calls are arranged so that the orientation of the surface is available when the wavefront routine is called. This is extremely useful in obtaining standard reflection parameters to investigate a

surface geometry without concurrent solution of the full laser variation required. This greatly speeds the task of investigating myriad and unusual mirror shapes.

The BOUNCE routine consists of three sections which may be mixed as desired by inserting jumps over unwanted sections. The first section calculates a normal elastic bounce. This was useful in testing certain notions of mirror properties without the added complication of the induced kick. The second section calculates a bounce including the kick. On each bounce it uses the current evanescent wave strength and direction to compute the bounce and kick. It also checks that the normal velocity is within allowable parameters. The third section calculates a random variation to simulate the gaussian spread in velocities due to the spontaneous nature of the force.

The gaussian spread simulation is worthy of further note. For each direction in the interaction reference frame, a random number is chosen between zero and one. This number is then used as the target in an iterative search which uses a ninth order polynomial expansion of the error function. The result is a random variable with a gaussian probability distribution. The root-mean-square deviation of the spread is then calculated based on the normal velocity and evanescent wave parameters. Multiplication of this sigma by the calculated random numbers gives a representative velocity shift for each direction. The velocity increments

are added in the interaction frame, but the effect in any frame is the same gaussian spread in velocity.

Program Use

When the program is run, it first checks the status of the line printer and asks for it to be turned on if desired. The program then prints out messages to identify the mirror shape, laser incidence parameters, and type of bounce the program is currently using. Each of the messages can be reprogrammed to aid in the identification of results.

The user is then asked for the starting height of the atom and the initial x, y, and z components of its velocity. The initial values of x and y are currently set a 0 (on axis), to preclude entry each time the program is run. This is easily changed to incorporate more flexibility, and all six components of the atom's position and velocity are printed in any event.

The next step in the program is the calculation of the apex position and energy. This serves as a reference and is printed after each bounce. The program then proceeds to find the next bounce position. It prints the elapsed time since the initial conditions, the bounce position, and the number of the bounce.

The program then prints the interaction parameters at the position of the bounce. These are the LASER intensity in watts, WX WY and WZ: the normalized components

of the incident wave vector, THETA: the laser's angle of incidence, R: the kick ratio, and IP and IC: the normalized components of the evanescent wave. These are defined Parallel and Complimentary to the projection of the atomic trajectory on the surface. Finally the DETUNING, including the Doppler contribution, is printed in units of Mhz.

The next output consists of SIGMA: the gaussian spread parameter, DN DP and DC: the random velocity deviations Normal to the surface and Parallel and Complimentary to the trajectory projection. The normal velocity of the atom is then printed for comparison with the maximum normal velocity permitted by the interaction parameters.

The SPEED, and the X Y and Z components of velocity before and after the bounce are then output. This allows a direct evaluation of the effects of the interaction. Finally, the apex energy and position are printed to show any shifts.

Program Listing

```
10 REM TRAP
20 PI=3.1415926530000001#
30 C=29979250000#      : REM CGS UNITS
40 GRAV=980.665
50 HBAR=1.0545*10^-27
60 OMEGA0=5.08985E+14 : REM SODIUM 3S1/2 TO 3P3/2
70 MASS=3.81729E-23    : REM SODIUM
80 RANDOMIZE 23382     : REM INITIALIZE FOR GAUSSIAN SPREAD
90 BOUNCE=0
100 FORM1$="&##.###            &######.##  &######.##
     &######.##  &##"
110 FORM2$="      &######.##  &######.##  &######.##  &######.##
     &#####.##"
120 FORM3$="&######.##&######.##&######.##"
130 FORM4$="&######.##  &#####.##"
140 PR=INP(230)        : REM CHECK PRINTER STATUS
150 PR=PR16
160 PRINTER=(PR/2-PR2)*2
170 IF PRINTER=1 OR FLAGPR=1 THEN 230
180 PRINT "Please Turn on the Printer (if desired), and
     press RETURN"
190 A$=INKEY$
200 IF LEN(A$)=0 THEN 190
210 FLAGPR=1
220 GOTO 140           :REM END OF PRINTER CHECK
230 TIME=0
240 X0=0
250 Y0=0
260 PRINT
270 IF NOT PRINTER=1 THEN 340 : REM NO PRINTER
280 GOSUB 1430 : REM SURFACE ROUTINE
290 LPRINT ZSURF$
300 GOSUB 1760 : REM WAVEFRONT ROUTINE
310 LPRINT WAVE$
320 GOSUB 2580 : REM BOUNCE ROUTINE
330 LPRINT BOUNCE$
340 INPUT;" Z0: ",Z0
350 INPUT;" VX: ",VX
360 INPUT;" VY: ",VY
370 INPUT " VZ: ",VZ
380 IF NOT PRINTER=1 THEN 430 : REM NO PRINTER
390 LPRINT
400 LPRINT USING FORM3$;"  X0: ";X0;"  Y0: ";Y0;"  Z0: ";Z0
410 LPRINT USING FORM3$;"  VX: ";VX;"  VY: ";VY;"  VZ: ";VZ
420 LPRINT
430 GOSUB 1340 : REM TRAJ ROUTINE
440 BSUBX=VX
450 BSUBY=VY
460 BSUBZ=VZ
470 GOSUB 2120 : REM APEX ROUTINE
480 T=0
```

```
490 DT=.01
500 GOSUB 1340 : REM TRAJ ROUTINE
510 GOSUB 1430 : REM MIRROR SURFACE
520 DZ=Z-ZSURF
530 T=T+DT
540 DZOLD=DZ
550 GOSUB 1340 : REM TRAJ ROUTINE
560 GOSUB 1430 : REM MIRROR SURFACE
570 DZ=Z-ZSURF
580 IF DZ>.01 THEN 530
590 IF ABS(DZ)<.01 THEN 670
600 DT=-DT*DZ/(DZ-DZOLD)
610 T=T+DT
620 DZOLD=DZ
630 GOSUB 1340 : REM TRAJ ROUTINE
640 GOSUB 1430 : REM MIRROR SURFACE
650 DZ=Z-ZSURF
660 GOTO 590   : REM NEXT STEP IN INTERCEPT SEARCH
670 TIME=TIME+T
680 BOUNCE=BOUNCE+1
690 PRINT
700 PRINT USING FORM1$;"TIME=";TIME;"  X=";X;" Y=";Y;" Z=";
    Z;"BOUNCE # ";BOUNCE
710 IF NOT PRINTER=1 THEN 740 : REM NO PRINTER
720 LPRINT
730 LPRINT USING FORM1$;"TIME=";TIME;"  X=";X;" Y=";Y;" Z=";
    Z;"BOUNCE # ";BOUNCE
740 GOSUB 830  : REM BOUNCE ROUTINE
750 GOSUB 2120 : REM APEX CALCULATION
760 X0=X
770 Y0=Y
780 Z0=Z
790 VX=BSUBX
800 VY=BSUBY
810 VZ=BSUBZ
820 GOTO 480   : REM RETURN TO FIND NEXT INTERCEPT

830 REM BOUNCE
840 GOSUB 1580 : REM MIRROR NORMAL
850 GOSUB 2040 : REM TRAJ VECTOR
860 GOSUB 1760 : REM WAVEFRONT ROUTINE
870 PRINT USING FORM2$;"LASER= ";INTE;"WX=";WSUBX;"WY=";
    WSUBY;"WZ=";WSUBZ
880 IF NOT PRINTER=1 THEN 900 : REM NO PRINTER
890 LPRINT USING FORM2$;"LASER= ";INTE;"WX=";WSUBX;"WY=";
    WSUBY;"WZ=";WSUBZ

900 REM TRANSFORMATION TO N,C,P COORDINATES
910 ADOTN=NORMX*NVX+NORMY*NVY+NORMZ*NVZ
920 ASUBX=NVX
930 ASUBY=NVY
940 ASUBZ=NVZ
950 REM DETERMINE OF P(ARALLEL) AND C(OMPLIMENTARY) VECTORS
```

```
960 THETAI=1
970 IF NOT (ADOTN >-1) THEN THETAI=0
980 IF THETAI = 0 THEN 1000 : REM AVOID NEGATIVE SQUARE ROOT
990 THETAI=ATN(-SQR(1-ADOTN^2)/ADOTN)
1000 ASUBN=-SPEED*COS(THETAI)
1010 ASUBP=SPEED*SIN(THETAI)
1020 ASUBC=0
1030 IF NOT (THETAI = 0) THEN 1110 : REM NORMAL INCIDENCE
1040 CSUBX=0 : CSUBY=1 : CSUBZ=0
1050 NORMPERP=SQR(NORMY^2+NORMZ^2)
1060 IF NORMPERP=0 THEN 1140 : REM NORM IS THE X AXIS
1070 CSUBX=0
1080 CSUBY=NORMZ/NORMPERP
1090 CSUBZ=-NORMY/NORMPERP
1100 GOTO 1140
1110 CSUBX=(ASUBY*NORMZ-ASUBZ*NORMY)/SIN(THETAI)
1120 CSUBY=(ASUBZ*NORMX-ASUBX*NORMZ)/SIN(THETAI)
1130 CSUBZ=(ASUBX*NORMY-ASUBY*NORMX)/SIN(THETAI)
1140 PSUBX=NORMY*CSUBZ-NORMZ*CSUBY
1150 PSUBY=NORMZ*CSUBX-NORMX*CSUBZ
1160 PSUBZ=NORMX*CSUBY-NORMY*CSUBX
1170 GOSUB 2260 : REM IMPULSE DIRECTION ROUTINE
1180 GOSUB 2580 : REM BOUNCE ROUTINE

1190 REM TRANSFORMATION BACK TO X,Y,Z
1200 BSUBX=BSUBN*NORMX+BSUBC*CSUBX+BSUBP*PSUBX
1210 BSUBY=BSUBN*NORMY+BSUBC*CSUBY+BSUBP*PSUBY
1220 BSUBZ=BSUBN*NORMZ+BSUBC*CSUBZ+BSUBP*PSUBZ
1230 SPEEDB=SQR(BSUBX^2+BSUBY^2+BSUBZ^2)
1240 A$="SPEEDA="
1250 B$="SPEEDB="
1260 C$="VNORMMAX= "
1270 D$="VNORM=     "
1280 PRINT USING FORM2$;A$;SPEED;"VX=";VX;"VY=";VY;"VZ=";
     DZDT;C$;VNORMMAX
1290 PRINT USING FORM2$;B$;SPEEDB;"BX=";BSUBX;"BY=";BSUBY;
     "BZ=";BSUBZ
1300 IF NOT PRINTER=1 THEN 1330 : REM NO PRINTER
1310 LPRINT USING FORM2$;A$;SPEED;"VX=";VX;"VY=";VY;"VZ=";
     DZDT;C$;VNORMMAX
1320 LPRINT USING FORM2$;B$;SPEEDB;"BX=";BSUBX;"BY=";BSUBY;
     "BZ=";BSUBZ
1330 RETURN

1340 REM TRAJ SUBROUTINE
1350 REM GIVEN X0,Y0,Z0
1360 REM GIVEN VX,VY,VZ,T
1370 REM RETURNS X,Y,Z,DZDT
1380 X=X0+VX*T
1390 Y=Y0+VY*T
1400 Z=Z0+VZ*T-GRAV*T*T/2
1410 DZDT=VZ-GRAV*T
1420 RETURN
```

```
1430 REM MIRROR SURFACE
1440 REM GIVEN X,Y
1450 REM RETURNS ZSURF
1460 HEIGHT=10
1470 PHI=ATN(.0187)
1480 PHID=PHI*180/PI
1490 Q=TAN(PHI)
1500 ZSURF=X*Q
1510 ZSURF=ZSURF+X^2/4/HEIGHT
1520 ZSURF=ZSURF+Q*X^3/4/HEIGHT^2
1530 ZSURF=ZSURF+(8*Q^2+1)*X^4/32/HEIGHT^3
1560 ZSURF$="Z = Four Term Expansion of Longitudinal Trap"
1570 RETURN

1580 REM MIRROR NORMAL
1590 REM GIVEN X,Y
1600 REM RETURNS NORMX,NORMY,NORMZ
1610 Q=TAN(PHI)
1620 DZDX=Q
1630 DZDX=DZDX+X/2/HEIGHT
1640 DZDX=DZDX+3*Q*X^2/4/HEIGHT^2
1650 DZDX=DZDX+(8*Q^2+1)*X^3/8/HEIGHT^3
1680 DZDY=0
1690 GOTO 1710                    : REM SKIP LATERAL FOCUS
1700 DZDY=ALPHA*Y/2/(HEIGHT-Z)    : REM LATERAL FOCUS 2
1710 LORM=SQR(1+DZDX^2+DZDY^2)
1720 NORMX=-DZDX/LORM
1730 NORMY=-DZDY/LORM
1740 NORMZ=1/LORM
1750 RETURN

1760 REM WAVEFRONT ROUTINE
1770 REM GIVEN X,Y,Z
1780 REM RETURNS WSUBX, WSUBY, WSUBZ, WSTRENGTH, INDEX,
       DELTA, EINA
1790 THETAZ=ATN(DZDX)
1800 THETAZ=THETAZ*180/PI
1810 THETAWAVE=45+THETAZ
1820 THETAZRAD=THETAWAVE*PI/180
1830 WSUBZ=SIN(THETAZRAD)
1840 WSUBX=COS(THETAZRAD)
1850 WSUBY=0
1860 WAVE$="45 Degree Incidence to Surface Upward"
1870 GOTO 1940                    : REM SKIP PIPE WAVEFRONT
1880 THETAZ=45+PHIRAMPD
1890 THETAZRAD=THETAZ*PI/180
1900 WSUBZ=COS(THETAZRAD)
1910 WSUBX=-SIN(THETAZRAD)
1920 WSUBY=0
1930 WAVE$="WSUBZ=COS(THETA)  WSUBX=-SIN(THETA)  WSUBY=0
       THETA="+STR$(THETAZ)
1940 INTENSITY=1                  : REM WATTS
```

```
1950 INTENSITY=INTENSITY*10^7 : REM CGS UNITS
1960 INDEX=1.5
1970 DELTA=5*10^9              : REM DETUNING
1980 OMEGA=OMEGA0+DELTA
1990 EINA=6.22E+07             : REM SODIUM
2000 THETAMIN=ATN(1/INDEX/SQR(1-1/INDEX^2))
2010 THED=THETAMIN*180/PI
2020 INTE=INTENSITY/10^7
2030 RETURN

2040 REM TRAJ VECTOR
2050 REM GIVEN X,Y,Z,T
2060 REM RETURNS SPEED,NVX,NVY,NVZ
2070 SPEED=SQR(VX^2+VY^2+DZDT^2)
2080 NVX=VX/SPEED
2090 NVY=VY/SPEED
2100 NVZ=DZDT/SPEED
2110 RETURN

2120 REM APEX CALCULATION
2130 REM GIVEN B VECTOR COMPONENTS
2140 REM RETURNS XAPEX,YAPEX,ZAPEX,ENERGYAP
2150 TAPEX=BSUBZ/GRAV
2160 TIMEAPEX=TIME+TAPEX
2170 XAPEX=X+BSUBX*TAPEX
2180 YAPEX=Y+BSUBY*TAPEX
2190 ZAPEX=Z+GRAV*TAPEX^2/2
2200 SPEEDAPEX=SQR(BSUBX^2+BSUBY^2)
2210 ENERGYAP=(SPEEDAPEX^2/2+GRAV*ZAPEX)/1000
2220 PRINT USING FORM2$;"ENERGY=";ENERGYAP;" X=";XAPEX;
     " Y=";YAPEX;" Z=";ZAPEX
2230 IF NOT PRINTER=1 THEN 2250 : REM NO PRINTER
2240 LPRINT USING FORM2$;"ENERGY=";ENERGYAP;" X=";XAPEX;
     " Y=";YAPEX;" Z=";ZAPEX
2250 RETURN

2260 REM IMPULSE DIRECTION
2270 REM GIVEN NORM, CVECT, PVECT, WVECT
2280 REM RETURNS IMPSUBP, IMPSUBC, RATIO
2290 NDOTW=NORMX*WSUBX+NORMY*WSUBY+NORMZ*WSUBZ
2300 THETA=0
2310 IF NDOTW=0 THEN 2330 : REM NORMAL LASER INCIDENCE
2320 THETA=ATN(SQR(1-NDOTW^2)/NDOTW)
2330 WPERX=WSUBX-NORMX*COS(THETA)
2340 WPERY=WSUBY-NORMY*COS(THETA)
2350 WPERZ=WSUBZ-NORMZ*COS(THETA)
2360 IMPSUBP=(WPERX*PSUBX+WPERY*PSUBY+WPERZ*PSUBZ)/
     SIN(THETA)
2370 IMPSUBC=(WPERX*CSUBX+WPERY*CSUBY+WPERZ*CSUBZ)/
     SIN(THETA)
2380 RATIO=INDEX*EINA*SIN(THETA)/2/DELTA/
     SQR(INDEX^2*SIN(THETA)^2-1)
2390 THETD=THETA*180/PI
```

```
2400 REM TEST ON EVANESCENT WAVE
2410 ALPHA=OMEGA*SQR(INDEX^2*SIN(THETA)^2-1)/C
2420 KWAVE=OMEGA*INDEX*SIN(THETA)/C
2430 THETAMIN=ATN(1/INDEX/SQR(1-1/INDEX^2))
2440 ESQUARE=128*PI*INDEX^2*COS(THETA)^2*INTENSITY/
     (INDEX^2-1)/(INDEX+1)^2/C
2450 MU=SQR(3/4*EINA*HBAR)*SQR((C/OMEGA0)^3)
2460 RABI=MU*SQR(ESQUARE)/HBAR
2470 DDT=DELTA+KWAVE*ASUBP*IMPSUBP
2480 TERM=2*MU^2/HBAR
2490 TERM=TERM*ESQUARE/HBAR
2500 TERM=TERM/(4*DDT^2+EINA^2)
2510 VNORMMAX=SQR(HBAR*DDT/MASS*LOG(1+TERM))
2520 PRINT USING FORM2$;"THETA= ";THETD;" R=";RATIO;"IP=";
     IMPSUBP;
2530 PRINT USING FORM4$;"IC=";IMPSUBC;"DETUNING= ";DDT/10^6
2540 IF NOT PRINTER=1 THEN 2570 : REM NO PRINTER
2550 LPRINT USING FORM2$;"THETA= ";THETD;" R=";RATIO;"IP=";
     IMPSUBP;
2560 LPRINT USING FORM4$;"IC=";IMPSUBC;"DETUNING= ";DDT/10^6
2570 RETURN

2580 REM BOUNCE ROUTINE
2590 BOUNCE$="Bounce without Impulse"
2600 BSUBN=-ASUBN
2610 BSUBP=ASUBP
2620 BSUBC=ASUBC
2630 BOUNCE$="Bounce with Impulse"
2640 BSUBN=-ASUBN
2650 BSUBP=ASUBP-2*RATIO*ASUBN*IMPSUBP
2660 BSUBC=ASUBC-2*RATIO*ASUBN*IMPSUBC
2670 REM GOTO 2710 : REM SKIP GAUSSIAN SPREAD
2680 BOUNCE$="Bounce with Impulse and Gaussian Spread"
2690 IF BOUNCE=0 THEN 3060
2700 GOTO 2716 :REM HIGH DETUNING
2702 SIGMAC=.2*SQR(BSUBN)
2704 SIGMAP=.455*SQR(BSUBN)
2706 SIGMANI=.05*BSUBN+.000012*BSUBN^3
2708 SIGMAN=SQR(SIGMAP^2+SIGMANI^2)
2710 GOTO 2730
2716 SIGMAC=.069*SQR(BSUBN)
2718 SIGMAP=.149*SQR(BSUBN)
2720 SIGMANI=.013*BSUBN+.0000016*BSUBN^3
2722 SIGMAN=SQR(SIGMAP^2+SIGMANI^2)
2730 TEMP=SQR(2/PI)
2740 FOR I=1 TO 3
2750 PROX=RND
2760 SPX=0
2770 DSPX=.1*SGN(PROX-.5)
2780 DPFIR=.5-PROX
2790 DPOLD=DPFIR
2800 IF NOT(SPX=0) THEN DPOLD=DP
```

```
2810 SPX=SPX+DSPX
2820 PROSP=.5+TEMP*(SPX/2-SPX^3/12+SPX^5/80-SPX^7/672+SPX^9/
     6912)
2830 DP=PROSP-PROX
2840 IF DP*SGN(DPFIR)>.01 THEN 2800
2850 IF ABS(DP)<.001 THEN 2910
2860 DSPX=-DSPX*DP/(DP-DPOLD)
2870 SPX=SPX+DSPX
2880 PROSP=.5+TEMP*(SPX/2-SPX^3/12+SPX^5/80-SPX^7/672+SPX^9/
     6912)
2890 DP=PROSP-PROX
2900 GOTO 2850 : REM NEXT ATTEMPT
2910 IF I=1 THEN DGAUN=SPX
2920 IF I=2 THEN DGAUP=SPX
2930 IF I=3 THEN DGAUC=SPX
2940 NEXT I
2950 DN=SIGMAN*DGAUN
2960 DP=SIGMAP*DGAUP
2970 DC=SIGMAC*DGAUC
2980 A$="SIGMAN="
2990 B$="UNORM=     "
3000 PRINT USING FORM2$;A$;SIGMAN;"DN=";DN;"DP=";DP;"DC=";
     DC;B$;BSUBN
3010 IF NOT PRINTER=1 THEN 3030 : REM NO PRINTER
3020 LPRINT USING FORM2$;A$;SIGMAN;"DN=";DN;"DP=";DP;"DC=";
     DC;B$;BSUBN
3030 BSUBN=BSUBN+DN
3040 BSUBP=BSUBP+DP
3050 BSUBC=BSUBC+DC
3060 RETURN
```

Z = Four Term Expansion of Longitudinal Trap
45 Degree Incidence to Surface Upward
Bounce with Impulse and Gaussian Spread

X0:	0.00	Y0:	0.00	Z0:	10.00				
VX:	10.00	VY:	10.00	VZ:	0.00				
	ENERGY=	9.91	X=	0.00	Y=	0.00	Z=	10.00	
TIME=	0.142		X=	1.42	Y=	1.42	Z=	0.09	BOUNCE # 1
	LASER=	1.00	WX=	0.64	WY=	0.00	WZ=	0.77	
	THETA=	45.00	R=	0.02	IP=	-0.25	IC=	0.97	DETUNING= 4999.96
	SIGMAN=	6.43	DN=	7.84	DP=	-0.13	DC=	0.12	VNORM= 139.78
	SPEEDA=	140.16	VX=	10.00	VY=	10.00	VZ=	-139.45	VNORMMAX= 455.52
	SPEEDB=	147.98	BX=	-10.54	BY=	9.91	BZ=	147.27	
	ENERGY=	11.03	X=	-0.16	Y=	2.91	Z=	11.14	
TIME=	0.443		X=	-1.75	Y=	4.40	Z=	0.05	BOUNCE # 2
	LASER=	1.00	WX=	0.75	WY=	0.00	WZ=	0.66	
	THETA=	45.00	R=	0.02	IP=	-0.04	IC=	1.00	DETUNING= 5000.00
	SIGMAN=	7.33	DN=	-9.37	DP=	2.73	DC=	-1.65	VNORM= 147.90
	SPEEDA=	148.24	VX=	-10.54	VY=	9.91	VZ=	-147.53	VNORMMAX= 455.52
	SPEEDB=	139.14	BX=	12.90	BY=	12.58	BZ=	137.97	
	ENERGY=	9.73	X=	0.07	Y=	6.17	Z=	9.75	
TIME=	0.724		X=	1.88	Y=	7.93	Z=	0.13	BOUNCE # 3
	LASER=	1.00	WX=	0.62	WY=	0.00	WZ=	0.78	
	THETA=	45.00	R=	0.02	IP=	-0.21	IC=	0.98	DETUNING= 4999.96
	SIGMAN=	6.25	DN=	-5.97	DP=	3.57	DC=	-0.27	VNORM= 137.97
	SPEEDA=	138.57	VX=	12.90	VY=	12.58	VZ=	-137.40	VNORMMAX= 455.52
	SPEEDB=	132.98	BX=	-13.51	BY=	16.01	BZ=	131.32	
	ENERGY=	8.97	X=	0.07	Y=	10.07	Z=	8.92	

VITA

Richard K. Hill was born on 9 January 1951 in South Charleston, West Virginia. He graduated from high school in Charleston, West Virginia, in 1969 and received the degree of Bachelor of Science from the University of Florida in June 1973. While in college, he wrote an article entitled "Electronic Stopping Cross Sections" which was published in Physics Review A in June 1973. He was an honor graduate of the Air Force Officers Training School in January 1974, and second in his class at Undergraduate Navigator Training at Mather AFB, California, in October 1974. He attended F-111 Weapons Systems Officer (WSO) training at Nellis AFB, Nevada, and was assigned to RAF Upper Heyford, England, in the F-111E. While there he served as a WSO and Instructor WSO responsible for aircrew training and European Theater Indoctrination. On assignment to Mountain Home AFB, Idaho, in October 1979, he served as an instructor WSO and Assistant Chief of Standardization and Evaluation. In July 1981, he was honored as the Tactical Air Command Instructor of the Year for 1980. He entered the School of Engineering, Air Force Institute of Technology, in June 1981.

Permanent Address: 4705 1st St NE, Apt 336
St Petersburg, FL 33703

UNCLASSIFIED

SECURITY CLASSIFICATION OF THIS PAGE *(When Data Entered)*

REPORT DOCUMENTATION PAGE		READ INSTRUCTIONS BEFORE COMPLETING FORM
1. REPORT NUMBER AFIT/GEP/PH/82D-13	2. GOVT ACCESSION NO.	3. RECIPIENT'S CATALOG NUMBER
4. TITLE *(and Subtitle)* ELECTROMAGNETIC MIRROR DYNAMICS		5. TYPE OF REPORT & PERIOD COVERED MS THESIS 6. PERFORMING ORG. REPORT NUMBER
7. AUTHOR*(s)* RICHARD K. HILL CAPTAIN USAF		8. CONTRACT OR GRANT NUMBER*(s)*
9. PERFORMING ORGANIZATION NAME AND ADDRESS AIR FORCE INSTITUTE OF TECHNOLOGY (AFIT/EN) WRIGHT-PATTERSON AFB OHIO 45433		10. PROGRAM ELEMENT, PROJECT, TASK AREA & WORK UNIT NUMBERS
11. CONTROLLING OFFICE NAME AND ADDRESS		12. REPORT DATE DECEMBER 1982 13. NUMBER OF PAGES 84
14. MONITORING AGENCY NAME & ADDRESS*(if different from Controlling Office)*		15. SECURITY CLASS. *(of this report)* 15a. DECLASSIFICATION/DOWNGRADING SCHEDULE

16. DISTRIBUTION STATEMENT *(of this Report)*

APPROVED FOR PUBLIC RELEASE; DISTRIBUTION UNLIMITED

17. DISTRIBUTION STATEMENT *(of the abstract entered in Block 20, if different from Report)*

18. SUPPLEMENTARY NOTES

Approved for public release: IAW AFR 190-17.

LYNN E. WOLAVER
Dean for Research and Professional Development
Air Force Institute of Technology (ATC)
Wright-Patterson AFB OH 45433

19. KEY WORDS *(Continue on reverse side if necessary and identify by block number)*

RESONANT RADIATION
LASER RADIATION
NEUTRAL ATOMIC BEAMS
ATOMIC DEFLECTION

20. ABSTRACT *(Continue on reverse side if necessary and identify by block number)*

The phenomena of resonant radiation pressure is studied as it applies to the reflection of two-level atoms from an evanescent wave. The basic mechanism is examined in detail. Three applications are proposed, analyzed, and compared to existing methods of neutral beam control. The first application is a beam conducting pipe which can contain and decelerate a beam of atoms. The second application is a parabolic nozzle which can collimate and focus a beam three orders of magnitude better than comparable resonant focusing. The third

DD FORM 1 JAN 73 1473 EDITION OF 1 NOV 65 IS OBSOLETE

UNCLASSIFIED

SECURITY CLASSIFICATION OF THIS PAGE *(When Data Entered)*

application is a macroscopic trap for slow atoms which allows laser-free observation of ~100 cm/s atoms for times measured in seconds. A computer code which tracks atomic trajectories through multiple reflections is included.


END
FILMED
6-83
DTIC